Modeling Injection and Extraction Wells for Seawater Desalination in SEAWAT

by

Kwun Lok YU

B.S., Northeastern University (2013)

Submitted to the Department of Civil and Environmental Engineering
in partial fulfillment of the requirements for the degree of

MASTER OF ENGINEERING IN CIVIL AND ENVIRONMENTAL ENGINEERING

at the

MASSACHUSETTS INSTITUTE OF TECHNOLOGY

June 2017

Author ..... Signature redacted ....
Department of Civil and Environmental Engineering
May 19, 2017

Certified by..... Signature redacted .....
E. Eric Adams
Senior Research Engineer
Lecturer of Civil and Environmental Engineering
Thesis Supervisor

Accepted by .... Signature redacted .....
Jesse H. Kroll
Professor of Civil and Environmental Engineering
Chairman, Graduate Program Committee

Modeling Injection and Extraction Wells for Seawater Desalination in SEAWAT

by

Kwun Lok YU

Submitted to the Department of Civil and Environmental Engineering
on May 19, 2017, in partial fulfillment of the
requirements for the degree of
MASTER OF ENGINEERING IN CIVIL AND ENVIRONMENTAL ENGINEERING

Abstract

Subsurface intakes and disposal systems are gaining interest for seawater desalination in comparison with the older open ocean intake/discharge systems that induce many environmental problems. Facilities using reverse-osmosis technology to desalinate seawater require stringent feed water quality to operate efficiently, and are particularly prone to membrane fouling when contaminants enter the system. Subsurface systems leverage coastal aquifers as natural filters, increasing the effective flow field for seawater extraction and brine disposal, and are proven to reduce impacts on the coastal environment. In this study, we developed groundwater models in SEAWAT, a three-dimensional finite difference groundwater model capable of simulating a varying-density environment, to learn about the interactions of seawater, brackish water, freshwater and brine due to extraction and injection activities, with salinities ranging from 0-70 PSU, and densities ranging from 1000g/L to 1050g/L. Two hypothetical desalination plants with freshwater production rates adequate to supply 750 people and 7500 people were simulated. Using simplified cross-sectional two-dimensional models, an optimal offshore location can be identified to implement subsurface intake systems to extract seawater closest to the coastline while minimizing impacts on existing freshwater storage from seawater intrusion. Models have also shown that for the same desalination plants, the coastal aquifer is more tolerant of brine injection than feedwater extraction; given that desalination plants typically have a 50% efficiency, half of the extracted seawater becomes freshwater, and only the remaining wasted brine is injected into the aquifer. A 2D test model with an expanded longshore domain, as well as a 3D test model with non-uniform properties in the longshore direction were also developed to test sensitivity when the longshore domain is changed.

Thesis Supervisor: E. Eric Adams
Title: Senior Research Engineer
Lecturer of Civil and Environmental Engineering

Acknowledgments

I would like to extend my gratitude to the following people who made this thesis possible:

Thank you Dr. E. Eric Adams, for his encouragement, patient guidance and insightful advice. Dr. Adams has contributed invaluable knowledge to this thesis, and has guided me to the right direction whenever needed, from inception to completion.

I would also like to thank my parents, Stella Wai Fan Chu and King Fai YU for their unconditional and continual support to pursue this program and my career plan to work in the United States. I am forever grateful for their encouragement, inspiration, and moral support.

Thank you to all my friends and classmates in the MIT Civil and Environmental Engineering M. Eng. program, for making this experience rewarding and unique. I wish everyone in the M. Eng. Environmental Engineering program to have greener pastures with whatever new opportunities life may bring.

Finally, thank you to everyone in the Environmental Fluid Mechanics group and MIT Parsons Laboratory, for their willingness to offer help and setting a welcoming atmosphere to work in.

Contents

1 Introduction **11**

1.1 Current seawater desalination technology 12

1.1.1 Open ocean intakes 12

1.1.2 Subsurface well systems 12

1.2 Motivation to study subsurface intakes 13

1.2.1 Seawater intrusion 13

1.2.2 Operation costs for subsurface intakes 14

1.2.3 Hydrogeological conditions 14

2 Literature Review **15**

2.1 Seawater desalination & subsurface intakes 15

2.1.1 Subsurface intakes for seawater reverse osmosis facilities: Capacity limitation, water quality improvement, and economics 15

2.1.2 Subsurface intake systems: Green choice for improving feed water quality at SWRO desalination plants, Jeddah, Saudi Arabia 17

2.2 Numerical groundwater modelling 18

2.2.1 Concepts and modeling of groundwater systems 18

2.2.2 The importance of density dependent flow and solute transport modeling 20

2.2.3 TIDAL boundaries in SEAWAT 22

3 SEAWAT Model Developement **25**

3.1 Implicit coupling 26

3.2 Model domain and input parameters 27
3.2.1 Hydraulic conductivity 28
3.2.2 Variable density flow package 29
3.2.3 Recharge 30
3.3 Ocean boundary 30
3.3.1 Extraction rates 30
3.3.2 Injection rates 31
3.3.3 Model domain visualization 31
3.4 Generating initial conditions 34
3.4.1 Transient stress period 34
3.4.2 Reaching steady state 34
3.5 Supplementary test models 36

4 Model results for seawater extraction **39**
4.1 Extraction rates and well locations 39
4.2 Head and salinity distribution 40

5 Model results for brine injection **47**
5.1 Injection rates and well locations 47
5.2 Brine, brackish, fresh water distribution 48

6 Results and Discussion **55**
6.1 Optimal locations for well systems 55
6.1.1 Extraction wells 55
6.1.2 Injection wells 57
6.2 Test models comparison 58
6.3 Future Projects 60

A SEAWAT VDF codes **61**

B SEAWAT Model Structure Flowchart **65**

List of Figures

2-1 Different setups of extraction well systems[16] 16
2-2 Plan view of the Fukuoka desalination plant[16] 17
2-3 Comparison of organic matter concentrations[7] 18
2-4 Illustration of the Ghyben-Herzberg relation in a coastal aquifer[4] . . 21
2-5 Comparison of results of constant density and variable density models[3]. 22
2-6 Average flux comparison for the 7 tidal test models[3] 24

3-1 Salinity profile with the lower 500 m^3/d extraction rate, year 2 28
3-2 Horizontal hydraulic conductivity for the model. 29
3-3 2D model visualization in USGS ModelMuse 31
3-4 Freshwater lens at 10 years of simulation 35
3-5 Freshwater lens at 30 years of simulation 35
3-6 Freshwater lens at 250 years of simulation 36
3-7 Summary of base model and two test models. 37

4-1 Salinity profile with the lower 500 m^3/d extraction rate, year 2 40
4-2 Salinity profile with the lower 500 m^3/d extraction rate, year 15 41
4-3 Salinity profile with the lower 500 m^3/d extraction rate, year 50 41
4-4 Head profile with the lower 500 m^3/d extraction rate, year 2 42
4-5 Head profile with the lower 500 m^3/d extraction rate, year 15 42
4-6 Head profile with the lower 500 m^3/d extraction rate, year 50 43
4-7 Salinity profile with the higher 5000 m^3/d extraction rate, year 2 . . . 43
4-8 Salinity profile with the higher 5000 m^3/d extraction rate, year 15 . . . 44
4-9 Salinity profile with the higher 5000 m^3/d extraction rate, year 50 . . . 44

4-10 Head profile with the higher 5000 m^3/d extraction rate, year 2 45
4-11 Head profile with the higher 5000 m^3/d extraction rate, year 15 45
4-12 Head profile with the higher 5000 m^3/d extraction rate, year 50 46

5-1 Salinity profile with the lower 250 m^3/d injection rate, year 2 49
5-2 Salinity profile with the lower 250 m^3/d injection rate, year 15 49
5-3 Salinity profile with the lower 250 m^3/d injection rate, year 50 50
5-4 Salinity profile with the higher 2500 m^3/d injection rate, year 2 50
5-5 Salinity profile with the higher 2500 m^3/d injection rate, year 15 51
5-6 Salinity profile with the higher 2500 m^3/d injection rate, year 50 51
5-7 Head profile with the higher 2500 m^3/d injection rate, year 2 52
5-8 Head profile with the higher 2500 m^3/d injection rate, year 15 52
5-9 Head profile with the higher 2500 m^3/d injection rate, year 50 53

6-1 Salinity time-series low extraction rate, 500 m^3/d 56
6-2 Salinity time-series high extraction rate, 5000 m^3/d 57
6-3 2D model, salinity time-series low extraction rate, 500 m^3/d, 1000m uniform longshore 58
6-4 3D model, salinity time-series local extraction rate, 500 m^3/d 59

B-1 Illustration of the Ghyben-Herzberg relation in a coastal aquifer[9] . . 66

List of Tables

2.1 Examples of desalination plants with subsurface intakes[16] 16
2.2 Seven simulations of different packages to specific tidal boundaries[17] 23

3.1 Aquifer parameters used in SEAWAT base model 32
3.2 Boundary conditions used in SEAWAT base model 33

Chapter 1

Introduction

Seawater desalination has become a popular choice to meet freshwater demand in many regions with limited freshwater supply and unreliable precipitation. In the first chapter, we will introduce some background information on seawater desalination and subsurface intakes.

Chapter 2 reviews and summarizes literatures supporting this study, first on seawater desalination and subsurface intakes and then articles related to numerical groundwater modeling.

Chapter 3 describes the development of the SEAWAT model, and introduces the modularity of MODFLOW, as well as details regarding the variable-density flow and transport equations.

Chapter 4 describes how the initial conditions are generating for both extraction and injection models. These initial conditions include a freshwater lens that is generated using a constant recharge rate from the top layer of the groundwater model.

Chapter 5 describes the simulations on brine injection, using two different injection rates.

Chapter 6 decribes the simulations on seawater extraction, with two different extraction rates.

Chapter 7 summarizes our observations from the model results, and discuss on aspects that may be further studied in future projects.

1.1 Current seawater desalination technology

Most desalination plants utilize either reverse-osmosis (RO) technology or a multi-stage-flash (MSF) process to produce freshwater. RO utilizes a semi-permeable membrane to remove ions (salt) and natural organic matters. MSF is a thermal distillation process where seawater is heated and the condensed water vapor is collected as freshwater. On average, each part of seawater produces roughly half a part of freshwater and half a part of rejected brine with approximately double the salinity of the feed seawater, giving a 50% production for a given feed water extraction rate.[2]

1.1.1 Open ocean intakes

Older desalination plants extract seawater from open ocean intakes and dispose the rejected waste brine to open ocean outfall. Open ocean designs generally have the lowest capital cost but can result in impacts to the marine environment. At the intake fish can be impinged on intake surface, and the problems are most severe in plants with high production rate. Open ocean intakes may have mesh to prevent fisheries from entering the pre-treatment facilities; however, larvae and microorganisms can still penetrate this mesh and contribute to fouling of membranes at desalination plants using reverse osmosis. For open ocean outfalls, depending on the performance of the desalination plant, the rejected brine may have a salinity 125-300% of the ambient water[19]. In cases where dilution the ambient tidal and discharge mixing is insufficient, a continuous discharge of such brine can produce pockets of high salinity water that is detrimental to marine life.

1.1.2 Subsurface well systems

An alternative to open ocean designs is subsurface extraction and injection wells in coastal aquifers. Intake water percolates through the aquifer and use the aquifer itself as a natural filter. This has been proven to drastically decrease microbes and fish entrainment, thus improving feed water quality and reducing the requirements

pre-treatment processes[21]. Injection wells can inject high salinity brine into deeper depths in coastal aquifers. In preferable conditions, the injected brine will percolate down-gradient towards the ocean. During the process, salts mix with the groundwater, thus providing a certain degree of dilution before the brine enters the ocean. The larger area which the brine flow into the ocean also helps to prevent localized pockets of high salinity water from developing. Although these systems have a higher capital costs, the implied environmental benefits and reduction in pre/post treatment requirements can bring a net positive gain in some cases.[16]

1.2 Motivation to study subsurface intakes

Feed water quality has a direct relation to the efficiency of the desalination process, removal of algae, and other natural organic matter is crucial as a pretreatment for the actual desalination processes, especially for reverse osmosis (RO) desalination systems where insufficient pretreatment can lead to membrane fouling.[1]

Open water intakes not only cause negative environmental impacts in coastal water bodies, but also increase the capital costs have for pretreatment facilities and operating costs for membrane conditioning. Subsurface intakes can mitigate both problems effectively by using coastal aquifers as a natural filter to remove a high percentage of algae, bacteria, organic matter and other substances that facilitate membrane fouling. This also allow the use of less sophisticated pretreatment designs and help to reduce the capital cost.[6]

1.2.1 Seawater intrusion

In certain non-ideal conditions however, subsurface systems can have potential negative environmental impacts. For example, many researchers have expressed concerns on seawater intrusion due to landward flux driven by extraction pumps. Seawater intrusion is the landward movement of seawater which intrudes on existing freshwater storage in coastal aquifers. Existing potable water mixes with the intruding seawater and becomes brackish water, conficting with the objective of

desalination to produce freshwater. Seawater intrusion can happen in both subsurface extraction and injection systems. In the case of brine injection, the high concentration gradient between brine and freshwater can be an even greater concern than the landward movement of seawater from extraction.[5]

1.2.2 Operation costs for subsurface intakes

The increased capital costs are also a significant obstacle for governments to implement such subsurface systems. However, studies have shown that the increased costs can be offset by the simplification of pretreatment facilities, and in the case of RO desalination plants, prolonging the average life of membranes. The long-term benefits incentivize newer desalination plants to adopt such subsurface intake systems; the state of California's coastal commission mandates the use of subsurface intakes for future desalination projects when feasible. And a desalination plant in Fukuoka, Japan, has been using a gallery-type subsurface intake system for the past 12 years and requires minimal maintenance of the membranes.[16]

1.2.3 Hydrogeological conditions

Another obstacle to implement such subsurface systems is locating coastal aquifers with the necessary hydrogeological conditions to support the flowrate for extraction and injection. Studies have found that the ideal coastal aquifers to have highly permeable geological formation, with hydraulic conductivity upwards of $40^{m}/_{d}$, and depth of 45m or deeper. If these requirements are not met, extraction wells may be incapable of pumping sufficient feed water to meet freshwater production rates, and injection wells may require much higher energy to inject the rejected brine from the desalination plants.[14].

Chapter 2

Literature Review

2.1 Seawater desalination & subsurface intakes

2.1.1 Subsurface intakes for seawater reverse osmosis facilities: Capacity limitation, water quality improvement, and economics

Missimer[16] discusses the environmental impacts of open-ocean intakes, and introduces the different set-ups and necessary hydrogeological conditions for subsurface intakes to perform as intended. The article also compiled a comprehensive list of RO desalination plants utilizing subsurface intakes for seawater extraction, shown in Table 2.1.

Various well configurations to implement the seawater extraction systems are introduced in the article; some examples, some of which as illustrated in Figure 2-1 are:

- Conventional Vertical Wells
- Angle Wells
- Horizontal Wells
- Radial Wells

Table 2
Selected seawater RO facilities using well intake systems.

Facility name	Location	Capacity[1] (m^3/d)	No. of wells
Sur	Oman	160,000	28
Alicante (combined for two facilities)	Spain	130,000	30
Tordera	Blanes, Spain	128,000	10
Pembroke	Malta	120,000	–
Bajo Almanzora	Almeria, Spain	120,000	14
Bay of Palma	Mallorca, Spain	89,600	16
WEB	Aruba	80,000	10
Lanzarote IV	Canary Islands, Spain	60,000	11
Sureste	Canary Islands, Spain	60,000	–
Blue Hills	New Providence I., Bahamas	54,600	12 (?)
Santa Cruz de Tenerife	Canary Islands, Spain	50,000	8
Ghar Lapsi	Malta	45,000	18
Cirkewwa	Malta	42,000	–
CR Aguilas, Murcia	Spain	41,600	–
SAWACO	Jeddah, Saudi Arabia	31,250	10
Dahab	Red Sea, Egypt	25,000	15
Turks & Caicos Water Company	Providenciales, Turks & Caicos Islands	23,260	6
Windsor Field	Bahamas	20,000	–
North Side Water Works	Grand Cayman	18,000	–
Ibiza	Spain	15,000	8
North Sound	Grand Cayman	12,000	–
Red Gate	Grand Cayman	10,000	–
Abel Castillo	Grand Cayman	9000	–
Al-Birk	Saudi Arabia	5100–8700	3
Lower Valley	Grand Cayman	8000	3
West Bay	Grand Cayman	7000	–
Britannia	Grand Cayman	5400	4
Bar Bay	Tortola, B.V.I.	5400	–
Morro Bay	California, USA	4500	5
Ambergris Caye	Belize	3600	–

[1] Capacity is for the well intake (approximated based on published reports or estimated based on the reported capacity of the plant divided by the reported recovery rate or a maximum of a 50% recovery rate where it is not reported).

Table 2.1: Examples of desalination plants with subsurface intakes[16]

(a) Slanted Well

(b) Radial Well

Figure 2-1: Different setups of extraction well systems[16]

A more unique type of configuration is a gallery intake design, that is feasible for coastal aquifers with lower hydraulic conductivity, with rates ranging from 2.4 to 9.6 $^{m}/_{d}$[16]. Gallery intake systems are usually closer to the seabed comparing to well systems, that provides an additional benefit to promote infauna growth due to accumulation of natural organic matter on the seabed, creating a nutrient-rich environment. One limitation to implement a gallery type system is to have a seabed that is relatively mud-free, as mud has a low conductance and restrict flow, such that

muddy sediments will become the bottleneck of the system.

A gallery type intake system has been in operation at a desalination plant in Fukuoka, Japan since 2005 (Figure 2-2). The plant has successfully demonstrated minimal cleaning of membranes, as well as minimal sediment dredging at the gallery intake seabed surface.

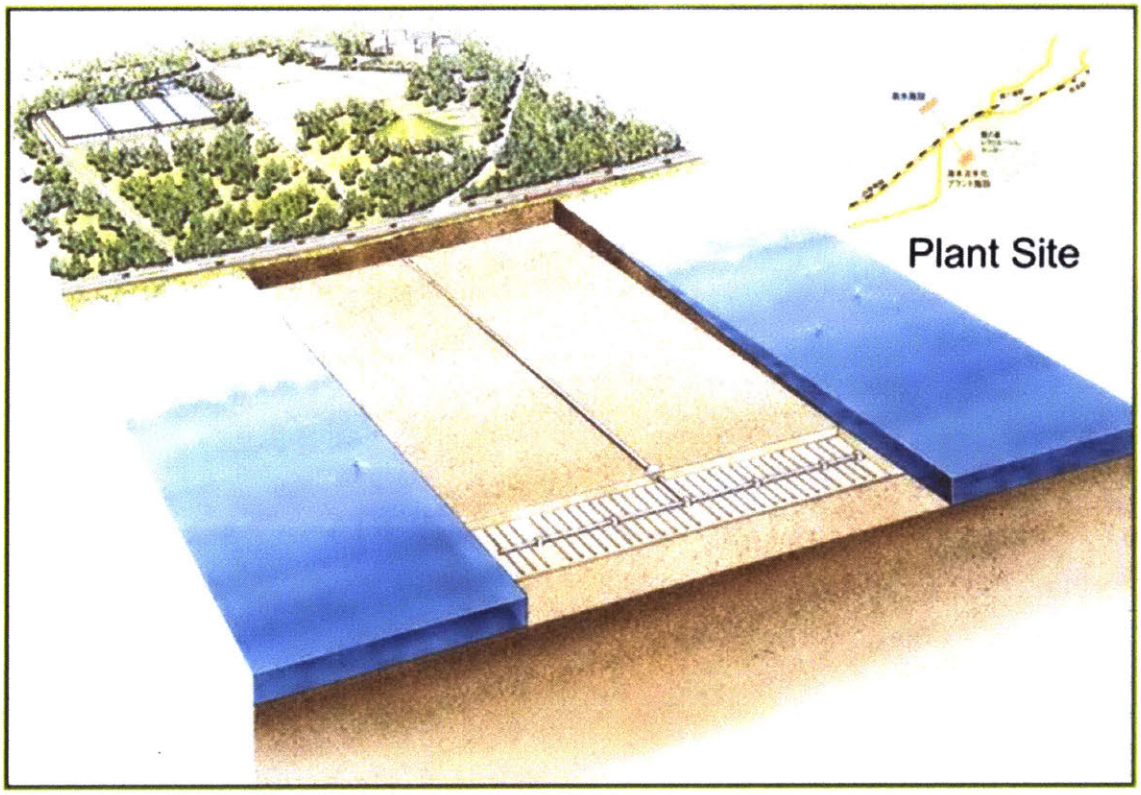

Figure 2-2: Plan view of the Fukuoka desalination plant[16]

2.1.2 Subsurface intake systems: Green choice for improving feed water quality at SWRO desalination plants, Jeddah, Saudi Arabia

Dehwah and Missimer[7] studied the performance of feed water quality control using subsurface intakes. Three desalination plants in Saudi Arabia were studied, showing results that up to 99% of the bacteria and between 84% to 100% of biopolymers within natural organic matter can be removed during the transport of seawater from

the ocean to the subsurface intakes. For the three locations, the concentrations of five natural organic carbons between seawater and extracted water from subsurface intakes were compared (Figure 2-3). Among the five natural organic carbons, biopolymers demonstrated the highest reduction percentage; biopolymers are the major organic carbon that causes membrane fouling.

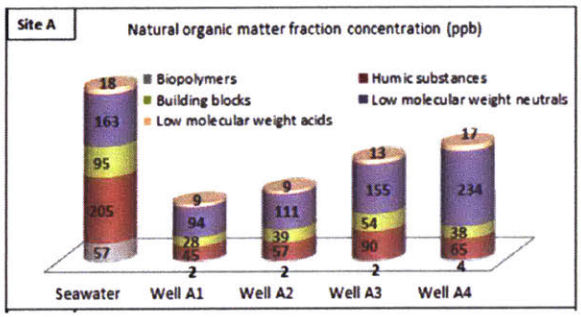

Figure 2-3: Comparison of organic matter concentrations[7]

2.2 Numerical groundwater modelling

2.2.1 Concepts and modeling of groundwater systems

Currently there are many available groundwater modeling software suitable for different hydrogeological conditions[10]. In the early phase of this study, we focused on comparing three different groundwater models to identify one that best suited our needs.

FEFLOW

Finite Element subsurface FLOW system, is a commercial groundwater modeling software developed by WASY GmbH and is currently owned by DHI, Inc. FEFLOW is capable of simulating flow in unsaturated and saturated zones, as well as performing solute transport calculation with variable densities. With a well-designed interface, FEFLOW is extremely powerful in data visualization, especially when modelers need to assimilate geographical datasets from Geographical Information Systems (GIS)[8]. The one major downside compared to the two other models is that the license is quite expensive, and for this study, we may not need for full capabilities of FEFLOW.

SUTRA

Saturated Unsaturated TRAnsport, is an open-source saturated-unsaturated groundwater flow and transport code developed by the USGS. Among the open-source models available, the biggest strength of SUTRA is its capability to simulate flow in unsaturated zones[20]. Flow and transport convergence criteria can be met easier than in other models that do not simulate unsaturated zones. This is especially true when there are fast adjustments in the phreatic surface level, and model grid cells may cycle quickly from wet to dry and vice versa. SUTRA can also check energy balances for groundwater models, it has been demonstrated that in some circumstances, mass may be conserved for a groundwater model whereas energy may not (Prof. Charles Harvey personal communication).

MODFLOW

MODFLOW is a three-dimensional (3-D) finite difference groundwater model developed by the USGS. It is one of the most popular groundwater models and is used widely around the world. USGS has provided significant effort in developing updates to improve the capabilities of the model, with the most current version releases in February 2017. MODFLOW uses a modular, or package input structure, making it easier for users to specify and incorporate different hydrogeological conditions; however, this may also cause compatibility issues when multiple packages are used. One significant disadvantage of MODFLOW is that its groundwater code can only simulate constant-density fluids, which is not sufficient for simulating variable-density interactions between seawater and freshwater.

ModelMuse

Even though MODFLOW can only simulate constant-density flow, it has well-documented functions published by the USGS and other researchers, that gave us incentives to use MODFLOW to learn about the basics of groundwater modeling.

For this part of the work, we used ModelMuse, a groundwater modeling graphical design interface developed by the USGS that supports multiple groundwater model, such as SUTRA, PHAST, MODFLOW, etc. Having a graphical interface greatly reduced the time required to set up different models, to vary parameters to test

sensitivity and to create useful graphics for data visualization.

USGS SWI2

USGS introduced the seawater intrusion package 2 (SWI2) for MODFLOW in 2013, to provide a simple numerical solution to simulate a sharp interface between seawater and freshwater zones. The package approximates density effects using equivalent freshwater heads and incorporates pseudo-source terms to the governing groundwater flow equations without having to solve the transport equations. However, since SWI2 does not solve the advective-dispersive transport equations, it cannot be used in circumstances where these processes are important. Another let down is that the only result from the SWI2 package is a sharp interface, providing minimal information about the distribution of salinity in the aquifer, especially in the brackish zone.

SEAWAT

To properly simulate variable-density groundwater flow, USGS developed SEAWAT, combining MODFLOW and MT3DMS. MT3DMS is a solute transport code that enables SEAWAT to simulate three-dimensional, variable-density, transient groundwater flow in porous media. Retaining the benefits of MODFLOW's modularity, models can still be designed with ease. Advective-dispersive transport equations can be optionally coupled with the groundwater flow equations, allowing modelers to run transient variable-density simulations.

2.2.2 The importance of density dependent flow and solute transport modeling

Barlow[4] provides a nice summary on how the difference in density between seawater and freshwater requires the use of a transient variable-density groundwater flow model (e.g. SUTRA, SEAWAT). The article contemplated if modelers can avoid using a variable-density model by calculating the freshwater equivalent head for seawater, using the Ghyben-Herzberg relation, also see below in Figure 2-4:

$$z = \frac{\rho_f}{\rho_s - \rho_f} h \tag{2.1}$$

$where\ h$ = Freshwater above sea level

z = Freshwater below sea level

ρ_f = Density of freshwater

ρ_s = Density of seawater

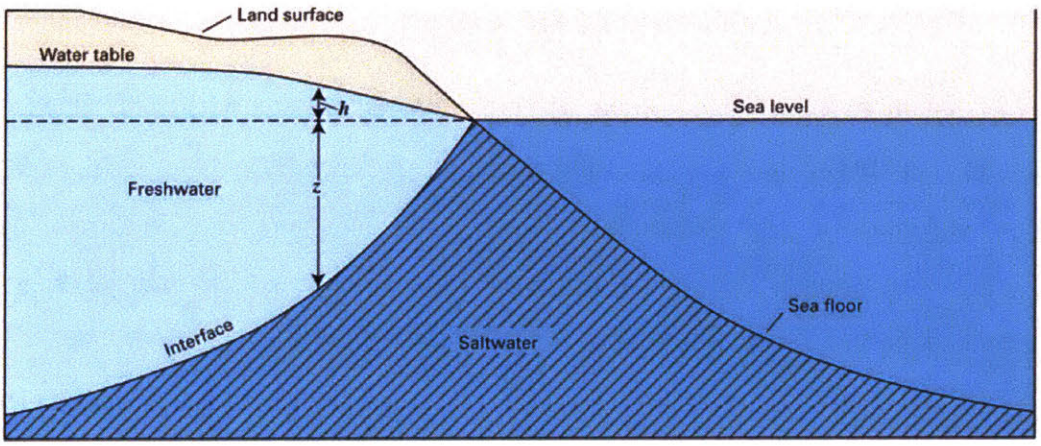

Figure 2-4: Illustration of the Ghyben-Herzberg relation in a coastal aquifer[4]

Figure 2-5 shows that the variable-density SEAWAT model demonstrates the closest match to the analytical solution as determined by the Ghyben-Herzberg interface. And the constant density, equivalent freshwater head MODFLOW model does not conform with the analytical solution at steady state.

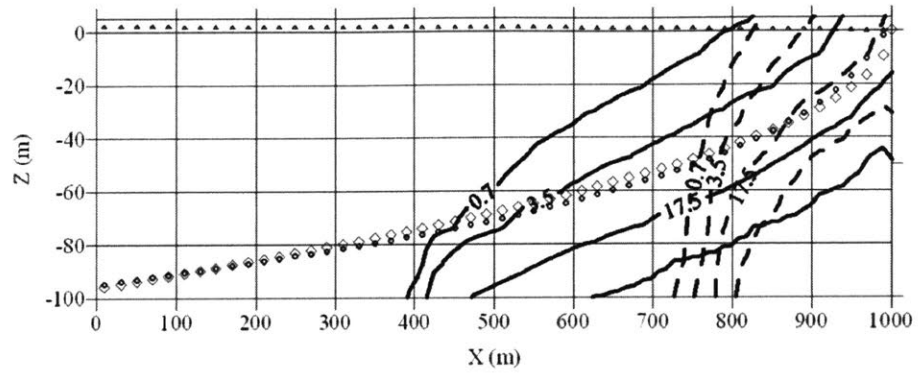

Figure 2-5: Comparison of results of constant density and variable density models[3]. Steady-state saline concentrations ($^{kg}/_{m^3}$) at Y = 250 m. of constant-density- (dashed line), variable- density model (solid line), Ghyben-Herzberg interface location (circles), and interface location based on Dupuit's assumptions (diamonds). Also shown is the phreatic water table (triangles).

2.2.3 TIDAL boundaries in SEAWAT

SEAWAT is an extended version of MODFLOW combined with MT3DMS, and retains the benefits of modularity using different packages[17]. But because of this modularity, modelers have various ways to specify the same hydrogeological condition. Mulligan[17] studies the performance of using different packages to simulate a realistic TIDAL boundary:

1) High Hydraulic-Conductivity (K) Zone : the ocean water body is modeled as an area with a significantly larger K value. This method allows SEAWAT to model the diffusion of submarine discharged freshwater through the seabed into the ocean, and simulate how the freshwater freshen ambient ocean water. However, the model is essentially treating the ocean water body as an aquifer with a high hydraulic conductivity, implying the flow calculation will not represent any actual mixing processes that may occur and should be ignored, this is because Darcy's law does not apply in surface water bodies.

2) As a boundary condition using General Head Boundary : The ocean is modeled as a boundary condition, implying the model will not simulate the interaction between

sub-marine discharged freshwater and the ambient ocean seawater. Intuitively this method is the most sensible, as it treats the entire ocean water body as one single unit, and that also help reducing simulation times.

3) As a boundary condition using Specified-Flux Boundary : Like a general head boundary, the ocean water body is treated as a single unit. For short period transient model, the specific water levels are important for simulating realistically, and can be input as a time-varying flux boundary condition.

Models with different combinations and settings of the three methods above have been developed, and are listed in Table 2.2.

Table 1
The Seven Approaches Used for Both the Beach and Tidal Flat Models

Simulation	Ocean Boundary Approach	Tidal Variation/Evaluation in Each Stress Period
1	High-*K*	Piece-wise linear
2	High-*K*	Constant (i.e., stepped tidal signal throughout tidal cycle)
3	GHB no DRN	Constant
4	GHB with DRN above coastal cells	Constant
5	GHB with DRN above and lateral to coastal cells	Constant
6	PBC only	Cosine
7	PBC with seepage	Cosine

Table 2.2: Seven simulations of different packages to specific tidal boundaries[17]

Interestingly, results show that all seven variations of simulating a tidal boundary have relatively similar performance, and the largest disagreement among the seven simulations occur during the peaks of tidal fluxes.

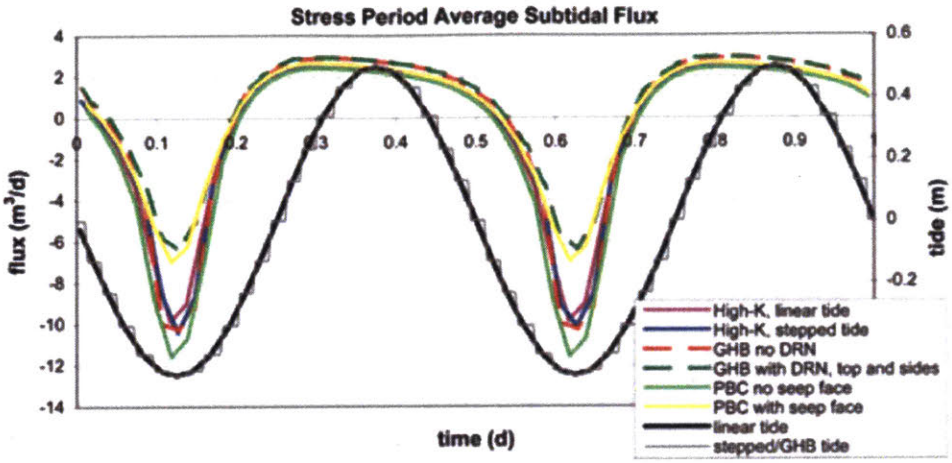

Figure 2-6: Average flux comparison for the 7 tidal test models[3]

Chapter 3

SEAWAT Model Developement

We decided to use SEAWAT for our study to simulate subsurface extraction and injection. Modelmuse was used for model development and results visualization. MODFLOW input files were then exported from Modelmuse and combined with the MT3DMS files. The model files were consolidated and the simulations were ran using SEAWAT codes. The governing flow and transport equations for SEAWAT are as below.

VDF Process solves the following form of the variable-density ground-water flow equation:

$$\nabla\left[\rho\frac{\mu_0}{\mu}K_0\Big(\nabla h_0+\frac{\rho-\rho_0}{\rho_0}\nabla z\Big)\right]=\rho S_{s,0}\frac{\delta h_0}{\delta t}+\theta\frac{\delta\rho}{\delta C}\frac{\delta C}{\delta t}-\rho_s q'_s \qquad (3.1)$$

$where\ \rho_0$ = freshwater density

μ = dynamic viscosity, not simulated in our model, $\frac{\mu_0}{\mu} = 1$

K_0 = hydraulic conductivity tensor

h_0 = freshwater head

$S_{s,0}$ = specific storage

t = time

θ = porosity

C = salinity

q'_s = sources or sink with density ρ_s

And the flow solutions are used to solve the solute transport equation:

$$\left(1 + \frac{\rho_b K_d^k}{\theta}\right) \frac{\delta(\theta C^k)}{\delta t} = \nabla\left(\theta D \nabla C^k\right) - \nabla\left(qC^k\right) - q'_s C_s^k \tag{3.2}$$

$where\ \rho_b$ = bulk density, $\frac{mass of solids}{total volume}$

K_d^k = distribution coefficient of salts, in $\frac{Length^3}{Mass}$

C^k = concentration of salts

h_0 = freshwater head

D = dispersion coefficient

q = darcy velocity

C_s^k = sources or sink of salts

3.1 Implicit coupling

The flow and transport equations are implicitly coupled, and will loop until user-defined convergence criteria are met (head, residual, number of loops, etc.). There are situations where head gradients are large enough (pumping wells with high extraction

rates) to cause simulation to be stuck in the coupled flow and transport loop, which may or may not result in termination of the simulation. To avoid this error, extraction rates would need to increased slowly instead of a sudden jump to avoid large changes in head gradients. Please refer to AppendixB-1 for the detailed procedures of SEAWAT.

3.2 Model domain and input parameters

For simplicity and to have better control over the input parameters, our base model is developed to simulate a two-dimensional (2D) setting, with the assumption that properties in the longshore direction are uniform. The model simulates 500m offshore (towards the left) to 1500m onshore (towards the right), with 200 grid cells, each 10m x 10m extending over the 2 kilometers in the cross-shelf direction. In the vertical direction, the model is irregularly discretized into 15 smaller layers reaching an elevation of 10m and a depth of 100m, with layers more concentrated towards sea level to help visualize the change in phreatic surface level. In the longshore direction, only one 10m layer is needed as we are simulating in a 2D setting.

To minimize the run times for the models, the 10m longshore layer represents 10% of a 100m coastline, as shown in the figure below, thus the input extraction and injection rates in the model should be divided by a factor of 10 from the real-world rates (e.g. 500 $^{m^3}/_{d}$ extraction rate has a modeled extraction rate of 50 $^{m^3}/_{d}$).

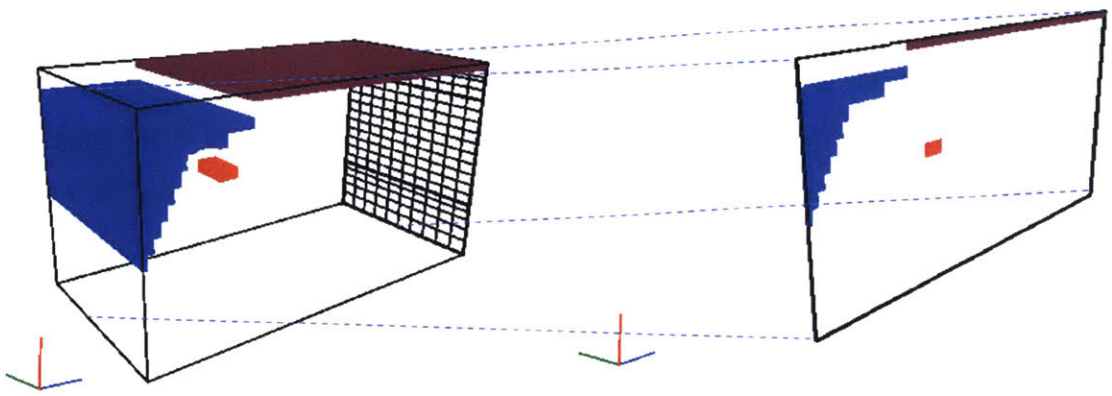

Figure 3-1: Salinity profile with the lower 500 $^{m^3}/_{d}$ extraction rate, year 2

3.2.1 Hydraulic conductivity

According to [16], the preferred coastal aquifer for subsurface extraction and injection should be in the range of fine sand, fractured dolomites or limestones. To match the properties of these materials, we chose a horizontal hydraulic conductivity of $40^{\mathrm{m}}/_{\mathrm{d}}$, from sea level to a depth of 70m. For depth below 70m, a horizontal hydraulic conductivity of $0.01^{\mathrm{m}}/_{\mathrm{d}}$ is used to simulate materials with low permeability, such as fine silt or clay.

The vertical hydraulic conductivity is 10 times less than the horizontal hydraulic conductivity.

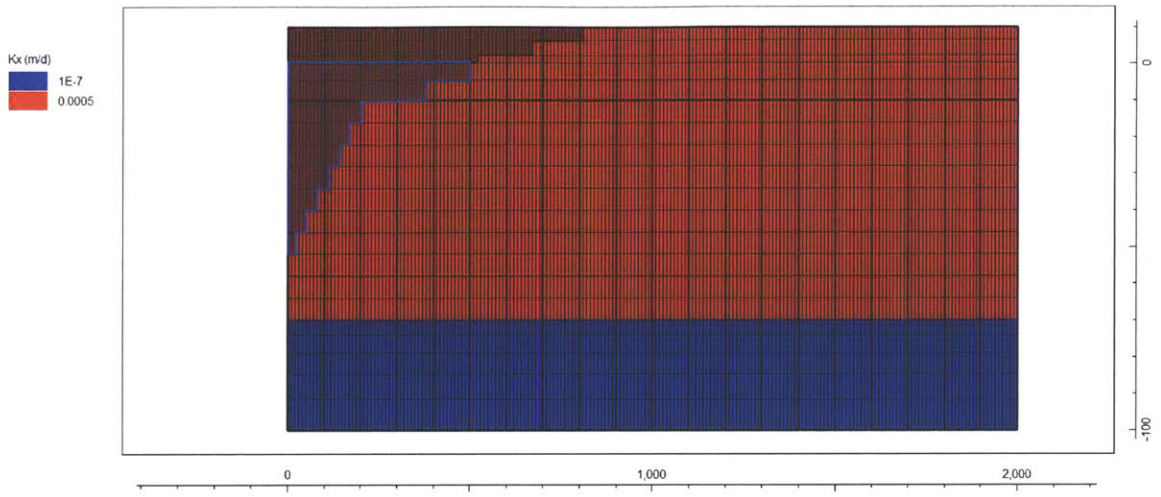

Figure 3-2: Horizontal hydraulic conductivity for the model.

3.2.2 Variable density flow package

As mentioned before, MT3DMS files are required in addition to the MODFLOW input files such that the simulation can be run using SEAWAT. The Variable Density Package is the MT3DMS package that governs the relation between the changing density of seawater, brackish water and freshwater. Freshwater has a density of 1000 g/L with a salinity of 0 PSU, and seawater has a density of 1025 g/L with a salinity roughly about 35 PSU. The linear relation has a slope of 0.7143, and this value is specified in the VDF package to calculate the density at a given salinity. Thus the equation of state relating salinity and density is:

$$\rho = \rho_0 + 0.714S \tag{3.3}$$

An example of the SEAWAT input file is included in Appendix A.

Although our models only considered changes in density influenced by salinity, it is possible to expand the equation of state to account for temperature changes, as well as ambient pressure such that the general equation of state will become:

$$\rho = \rho_0 + \frac{\delta\rho}{\delta C}\Big(C - C_0\Big) + \frac{\delta\rho}{\delta T}\Big(T - T_0\Big) + \frac{\delta\rho}{\delta P}\Big(P - P_0\Big) \tag{3.4}$$

3.2.3 Recharge

The main source of freshwater is distributed over the top active layer as recharge into the aquifer, given by:

$$\begin{aligned} Recharge &= Infiltration + GroundwaterInflow \\ &\quad - Evapotranspiration - Runoff \end{aligned}$$

and approximated to have a value of 0.47 $^{m}/_{year}$.

3.3 Ocean boundary

As the simulations in this study span a period of 50 years, tidal processes have minimal impact comparing to the processes within the coastal aquifer. As such, we modeled the ocean water body as a general head boundary (GHB) at 0 m (sea level) with a constant salinity of 35 PSU. According to [17], GHB simplifies the set-up of the model and reduces the run time of the simulation.

3.3.1 Extraction rates

Two pumping rates of 500 $^{m^3}/_{d}$ and 5000 $^{m^3}/_{d}$ were used to simulate the interaction of seawater and freshwater at different extraction rates. The models for this study were developed in 2D, with a 10m longshore grid layer to simulate a 100m longshore coastline. Hence the two listed pumping rates are scaled by a factor of 10 at 50 $^{m^3}/_{d}$ and 500 $^{m^3}/_{d}$. California water boards suggest that an average person in the state of California consumes about 90 gallons per day[18]. With a freshwater production efficiency of 50%, the specified extraction rates can provide adequate water supply to about 750 people and 7,500 people respectively. The modeled extraction rate

is distributed over a 10m longshore length with 10 perforations in the cross-shelf direction, in 10m intervals.

3.3.2 Injection rates

Only half of the extracted seawater becomes waste brine, and thus the injection rate when simulated is half of the specified pumping rate at 250 $^{m^3}/_{d}$ and 2500 $^{m^3}/_{d}$ respectively. However, the salinity of the injected waste brine has a salinity two times that of the feed water salinity at 70 PSU.

3.3.3 Model domain visualization

Figure 3-3 shows the actual model domain and boundary conditions, the blue grids depict the ocean boundary and slope, the red grids depict where the extraction or injection well may be located in the domain, and the purple grids depict the top layer with a constant recharge. Table 3.1 and 3.2 summarize the above modeled aquifer properties and boundar conditions, with reference to the associated SEAWAT packages used.

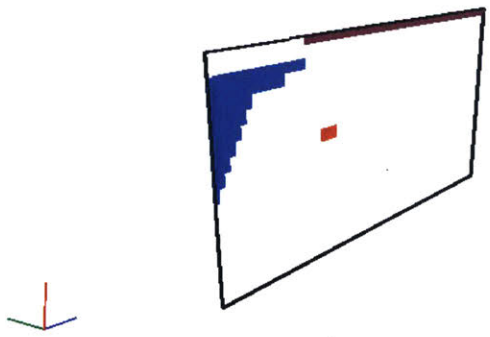

Figure 3-3: 2D model visualization in USGS ModelMuse

Table 3.1: Aquifer parameters used in SEAWAT base model

Parameter Description		
Hydraulic Conductivity $^{m}/_{d}$		**Comment**
Zone 1(0 - 70m deep)	0.0002	Represent hydraulic,conductivity in ranges of fine sand, or fractured limestone
Zone 2(70 - 100m deep)	1E-7	Represent hydraulic,conductivity of bedrock or an impermeable layer
Porosity (unitless)		
Uniform value	0.2	Assumed porosity of porous limestone similar to specific yield estimated by [15]
Dispersivity (m)		
Longitudinal	10	[11]
Transversal	1	

Table 3.2: Boundary conditions used in SEAWAT base model

Boundary Description		
Model perimeter		**Comment**
Bottom of bedrock layer, Zone 2	No-Flow	
Right Inland Boundary	No-Flow	
Left boundary beneath seafloor	No-Flow	
Ocean Boundary	GHB	General Head Boundary Package
Head (m), sea level	0	GHB allows movement into and from the ocean boundary depending on inland water levels
Conductance $^{m^2}/_{s}$	0.025	Hydraulic conductance of the interface(sediment) between the aquifer cell and the boundary
Salinity (PSU)	35	Constant salinity, ocean boundary as a source
Recharge	RCH	Recharge Package
Recharge Rate	1.5E-8 $^{m}/_{s}$	about 0.47 $^{m}/_{year}$
Uppermost active layer		phreatic surface, uniform over a 1500m crosshelf x 10m longshore area
Salinity (PSU)	0	Freshwater supply from recharge
Extraction/Injection Wells	WEL	Well Package
Extraction, low ($^{m^3}/_{s}$)	0.0006	Multiply value by 10 to get real-world value due to 2D scaling in longshore direction
Extraction, high ($^{m^3}/_{s}$)	0.006	Multiply value by 10 to get real-world value due to 2D scaling in longshore direction
Injection, low ($^{m^3}/_{s}$)	0.0003	Multiply value by 10 to get real-world value due to 2D scaling in longshore direction
Injection, high ($^{m^3}/_{s}$)	0.003	Multiply value by 10 to get real-world value due to 2D scaling in longshore direction

3.4 Generating initial conditions

The first step of simulating the brine injection and seawater extraction is to determine a proper initial condition that should match the existing condition of the coastal aquifer. The freshwater zone, brackish water zone and seawater zone should reach an equlibrium in terms of flow and salinity. A freshwater lens is created starting near the coastline and sloping downward towards inland, and the depth of the lens is governed by the hydrogeological conditions of the aquifer, specifically the hydraulic conductivity of the aquifer material.

3.4.1 Transient stress period

The model to generate the initial condition was run with a stress period of 1000 years, and it was determined from the model results that a steady-state was reached in about 200 years of the simulation. An initial salinity of 35 PSU is used to help accelerate the development of the freshwater lens, with a goal to reduce simulation runtime. Thus this 200-year time period should not be used as reference to what may happen in real world setting.

3.4.2 Reaching steady state

Below are three selected timesteps of the model showing the development of the freshwater lens and salinity distribution. Freshwater is being recharged from the top layer, and then infiltrates into the coastal aquifer before being discharged from the saturated zone and into the ocean. The denser seawater sinks towards the bottom of the aquifer and mixes with the infiltrating freshwater resembling a counterclockwise rotational motion to develope a brackish water zone, with the envelope of the brackish water zone increasing towards inland. The water table profile agress with the Ghyben-Herzberg relation (2.1).

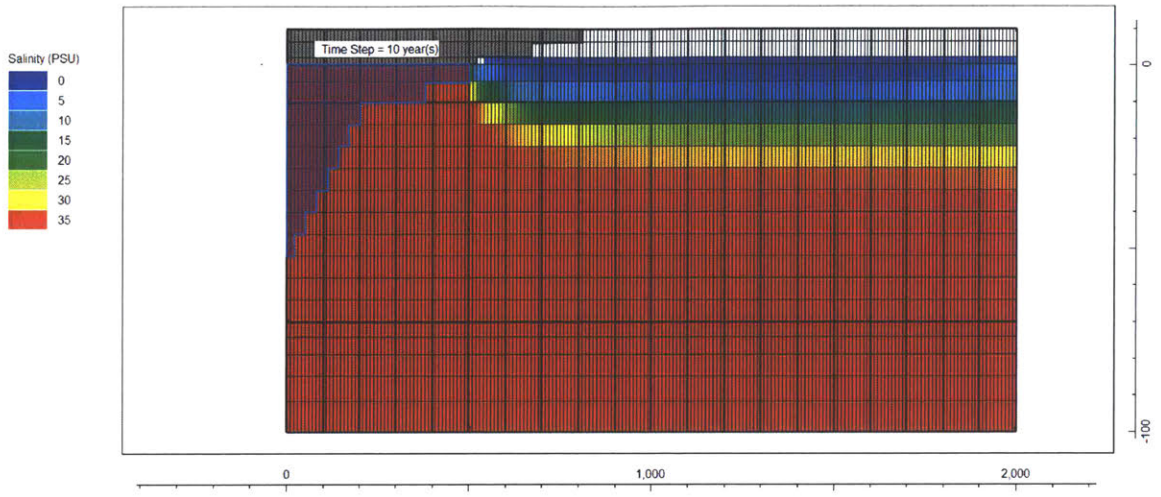

Figure 3-4: Freshwater lens at 10 years of simulation

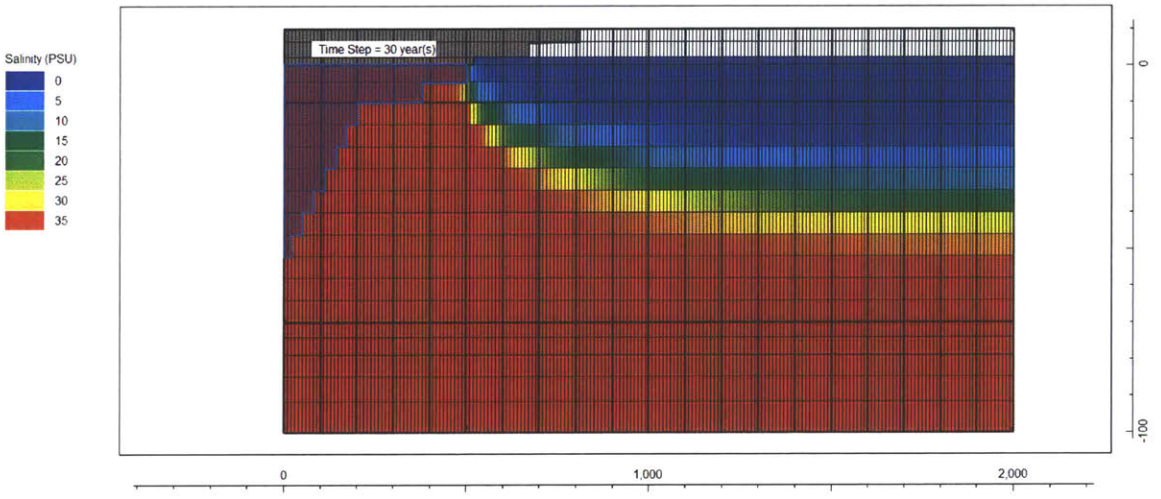

Figure 3-5: Freshwater lens at 30 years of simulation

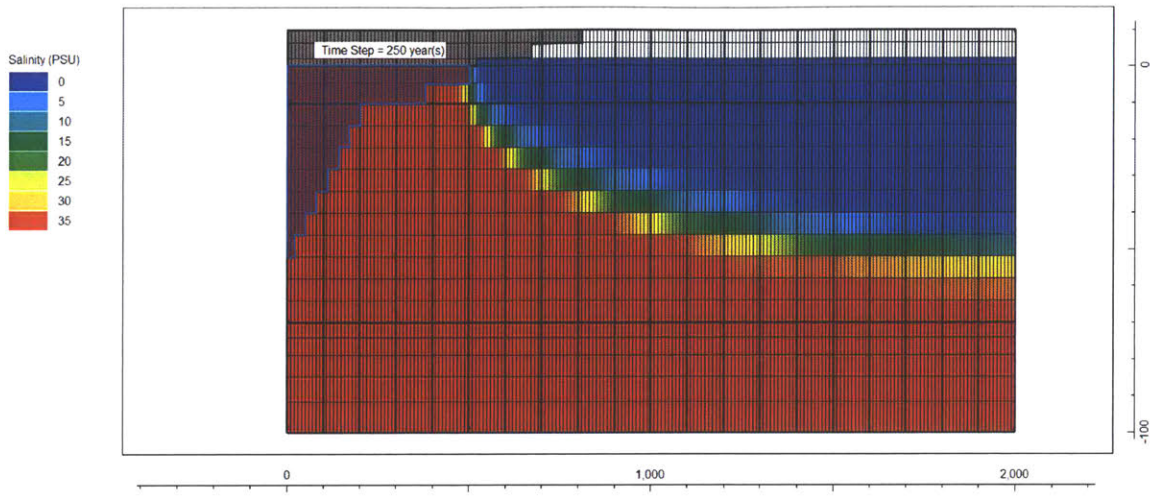

Figure 3-6: Freshwater lens at 250 years of simulation

3.5 Supplementary test models

Two additional test models were developed to compare how the model results will differ when the model domain has changed. In the base model mentioned above, seawater is extracted in a 10m (longshore)x 100m (cross-shelf) zone at a modeled extraction rate of 50 $^{m^3}/_{d}$. This is identical to a model with a 100m longshore length with a modeled extraction rate of 500 $^{m^3}/_{d}$. The recharge over the top layer of the domain is about $0.47^{m}/_{yr} \times 15000m^2 \div 365^{d}/_{yr} \approx 20^{m^3}/_{d}$. Since the recharge rate ($20^{m^3}/_{d}$) is lower than the extraction rate ($50^{m^3}/_{d}$), at inland locations, all of the recharged freshwater will be extracted, and the extracted flow will reach of about 22 PSU based on the conservation of salt mass:

$$Q_{seawater} \times C_{seawater} + Q_{recharge} \times C_{recharge} = Q_{extraction} \times C_{extraction} \tag{3.5}$$

In the first test model, we expanded the longshore domain to 1000m, represented by 100 grids, each 10m wide, hence essentially increasing the recharge rate by 100 times to 2000 $^{m^3}/_{d}$. The extraction rate used in this test is increased to 500 $^{m^3}/_{d}$ (an increase of 10 times), with wells uniformly distrubuted like the base model. Notice

that the recharge rate in this model is higher than the extraction rate; thus the freshwater storage should not experience significant depletion. While this is true, this scenario is also unrealistic to a moderate extent, as there would be no demand for seawater desalination if the groundwater is being recharged at such a high rate The model is basically for testing purposes.

In the second test model, we want to visualize an actual 3D model, where the longshore extraction rates are not uniform. In this model, the longshore domain is set at 100m, represented by 10 grids, each 10m wide. Recharge is set at 200 $^{m^3}/_{d}$, with an extraction rate of 50 $^{m^3}/_{d}$. The wells for this model are located only at locations mid-width in the longshore distance, spaning an area of 10m longshore x 100m crossshelf. Althrough the recharge rate is still higher than the extraction rate, the recharge zone is distrubted over an area much larger than that for extraction.

Figure 3-7 shows a summary of the base model and the two test models. Results for the two tests models are further discussed in Chapter 6.

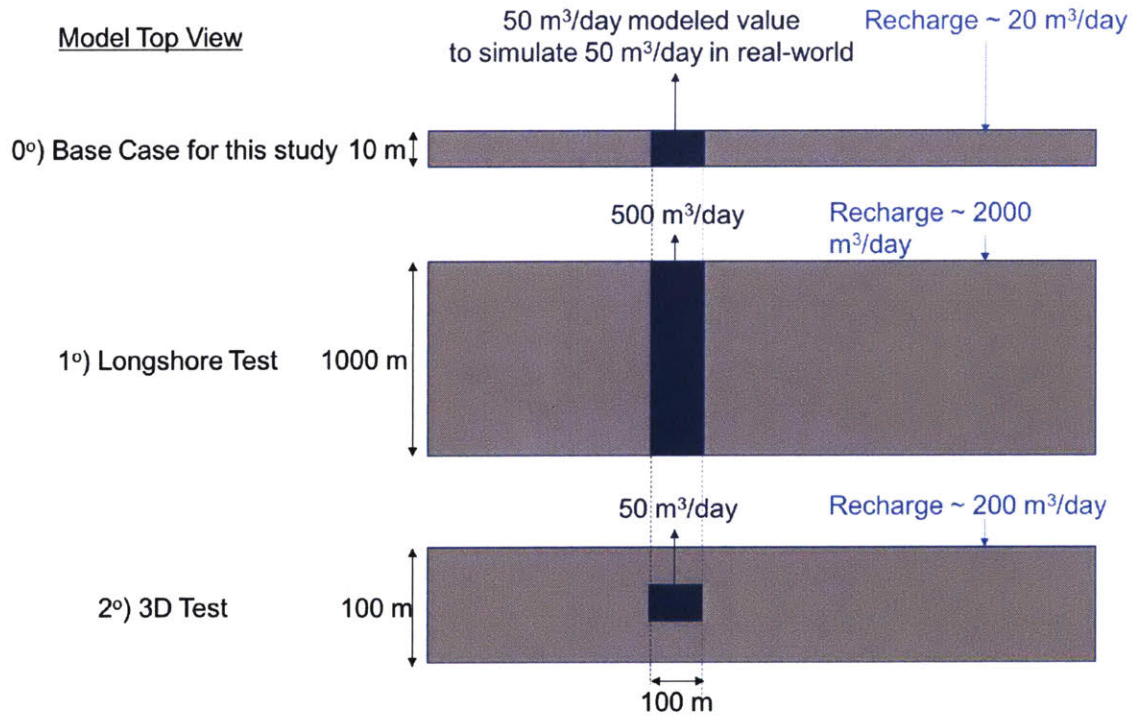

Figure 3-7: Summary of base model and two test models.

Chapter 4

Model results for seawater extraction

The MODFLOW well-package is used to model the extraction pumps. 10 pumps were modeled across a 100m distance in the cross-shelf direction to simulate a single pump extracting from a well with 10 perforations. Using the initial condition of an existing freshwater lens, the model was ran for a total of 51 years, with one year of warm-up period with no extraction, followed by 50 years of continuous extraction.

4.1 Extraction rates and well locations

Extraction rates were determined based on two hypothetical desalination plants with freshwater production rates of 250 m^3/d and 2500 m^3/d. With a production efficiency of 50%, this requires extraction rates of 500 m^3/d and 5000 m^3/d respectively to sustain the operations of the desalination plant. For the model with the higher extraction rate, the model experienced multiple occasions where the simulation was terminated because the convergence criteria could not be met by solving the coupled flow and transport equations. The problem was remedied by gradually increasing the extraction rate during the first year of extraction, such that extreme head gradients due to extraction can be reduced.

A total of 10 simulations were run for each extraction rate by choosing 10 extraction locations across the cross-shelf direction as shown in the next section.

4.2 Head and salinity distribution

Figures 4-1 to 4-12 show the freshwater heads and salinities at three timesteps for the two extraction rates. By looking at the salinity distribution, it may seem like water is extracted from below, with a tail of brackish water that routes towards the freshwater lens with a U shape routing. We could not identify the cause for this tail along with the pocket of water with higher salinity between the extraction pump and the freshwater lens. However, compaing with the head distributions, the results are more sensible, showing a radial pattern of negative heads directed towards the extraction well. As such, we contemplate that the seawater pocket as seen in the salinity distributions may be related to the mixing and density differences of the seawater intruding from the ocean and freshwater extracing from the freshwater lens.

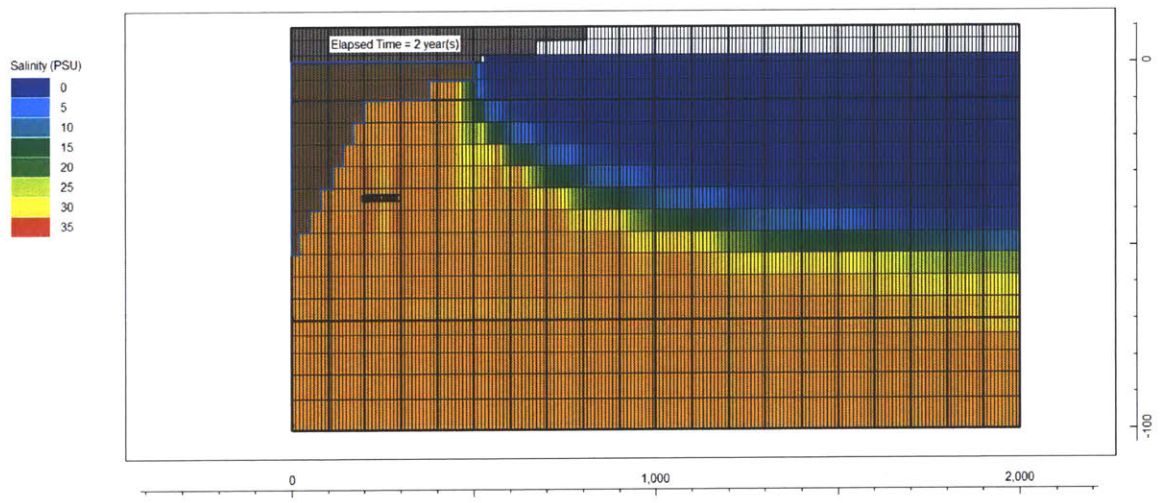

Figure 4-1: Salinity profile with the lower 500 $^{m^3}/_{d}$ extraction rate, year 2

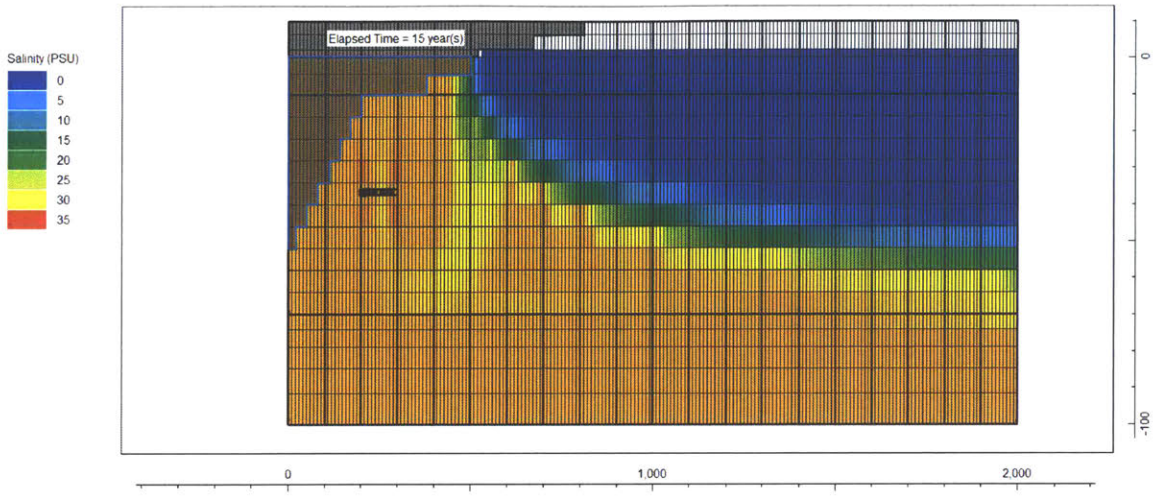

Figure 4-2: Salinity profile with the lower 500 $^{m^3}/_{d}$ extraction rate, year 15

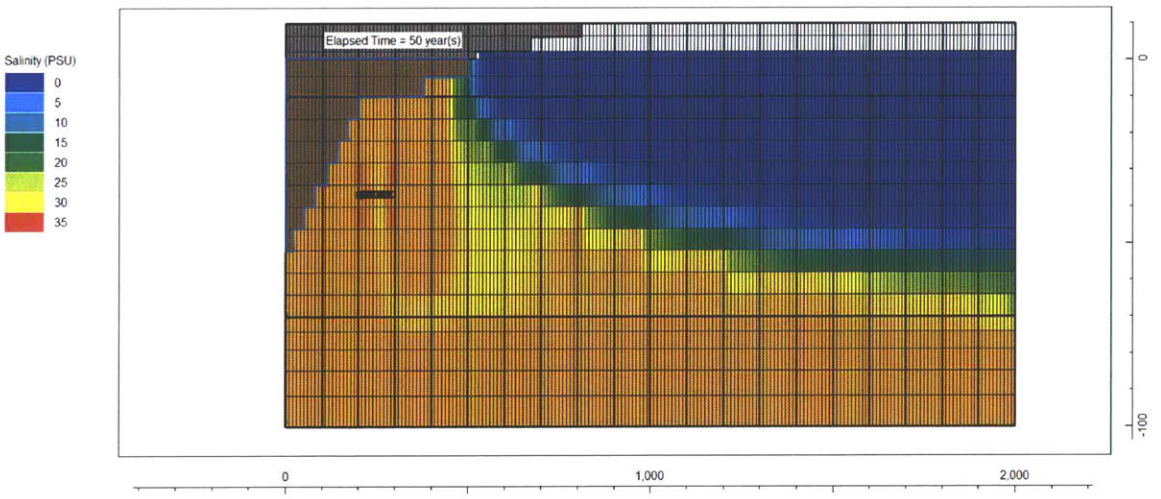

Figure 4-3: Salinity profile with the lower 500 $^{m^3}/_{d}$ extraction rate, year 50

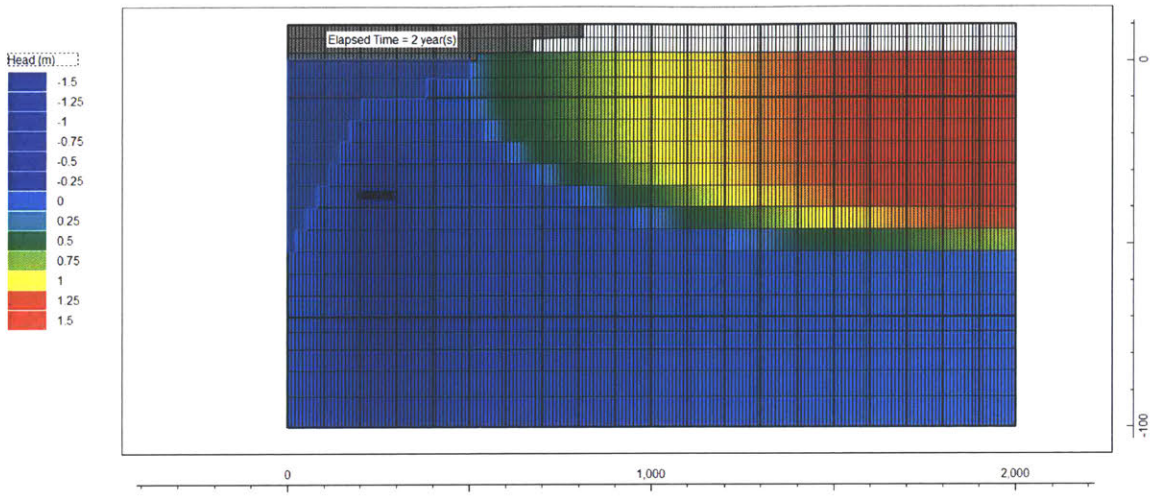

Figure 4-4: Head profile with the lower 500 m^3/d extraction rate, year 2

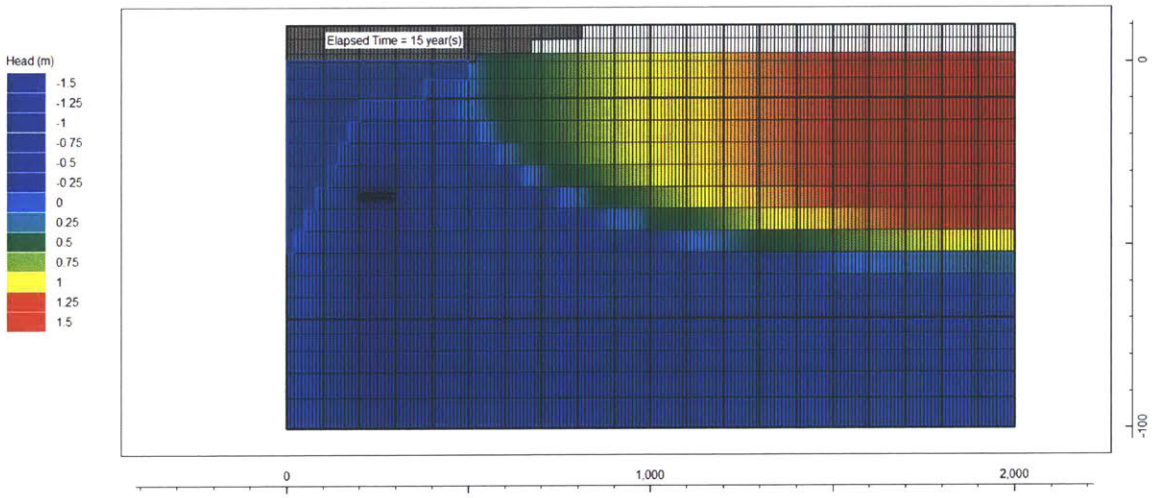

Figure 4-5: Head profile with the lower 500 m^3/d extraction rate, year 15

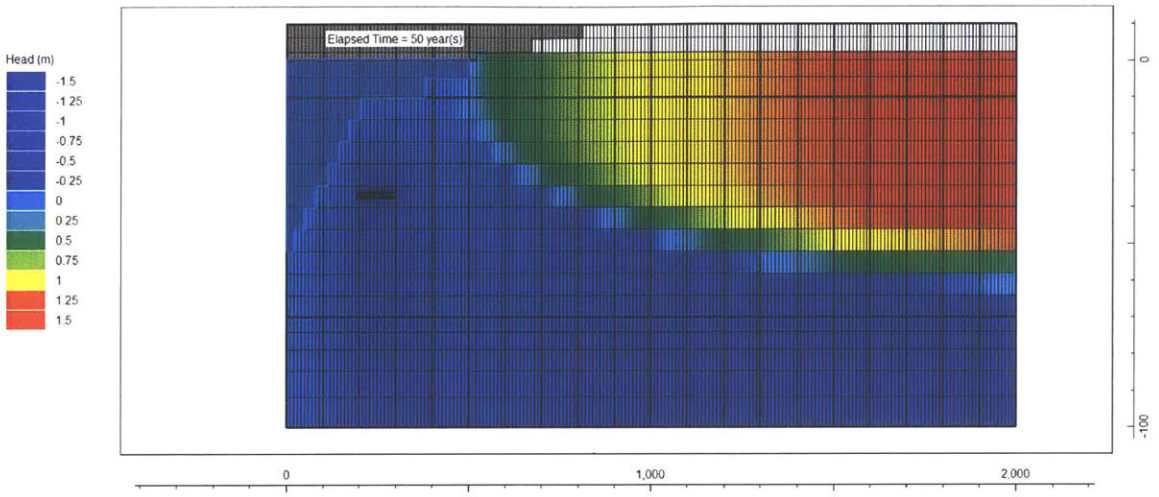

Figure 4-6: Head profile with the lower 500 $^{m^3}/_{d}$ extraction rate, year 50

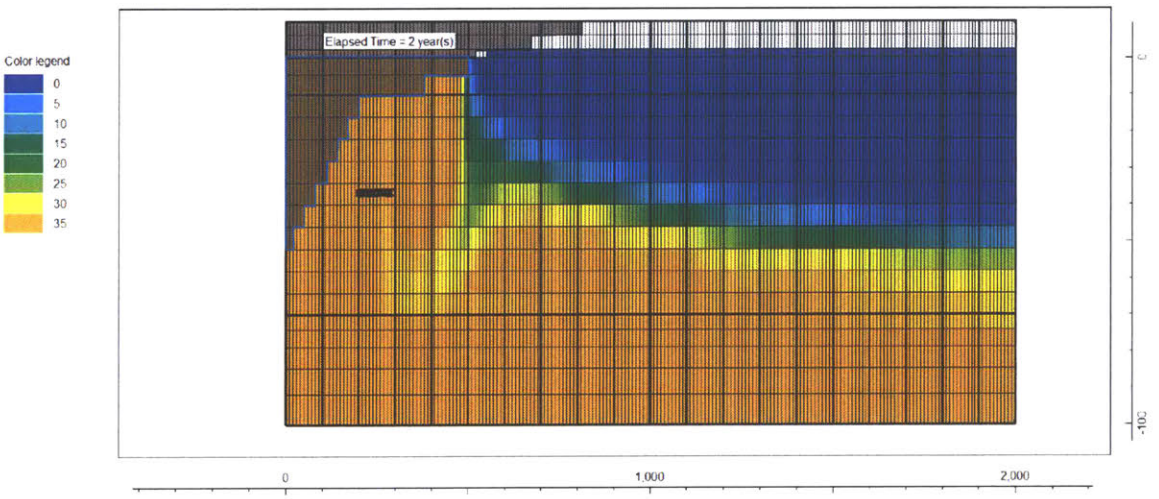

Figure 4-7: Salinity profile with the higher 5000 $^{m^3}/_{d}$ extraction rate, year 2

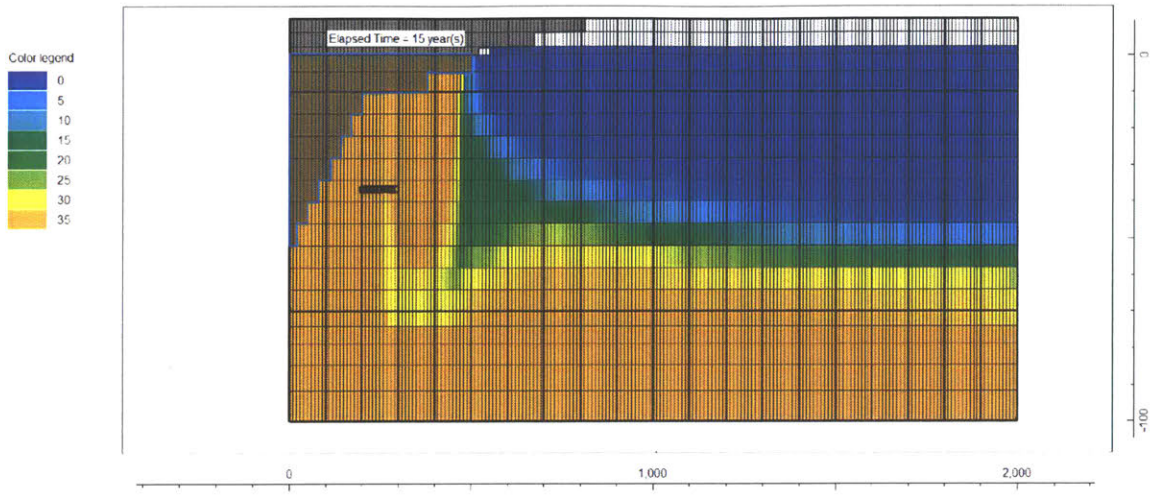

Figure 4-8: Salinity profile with the higher 5000 m^3/d extraction rate, year 15

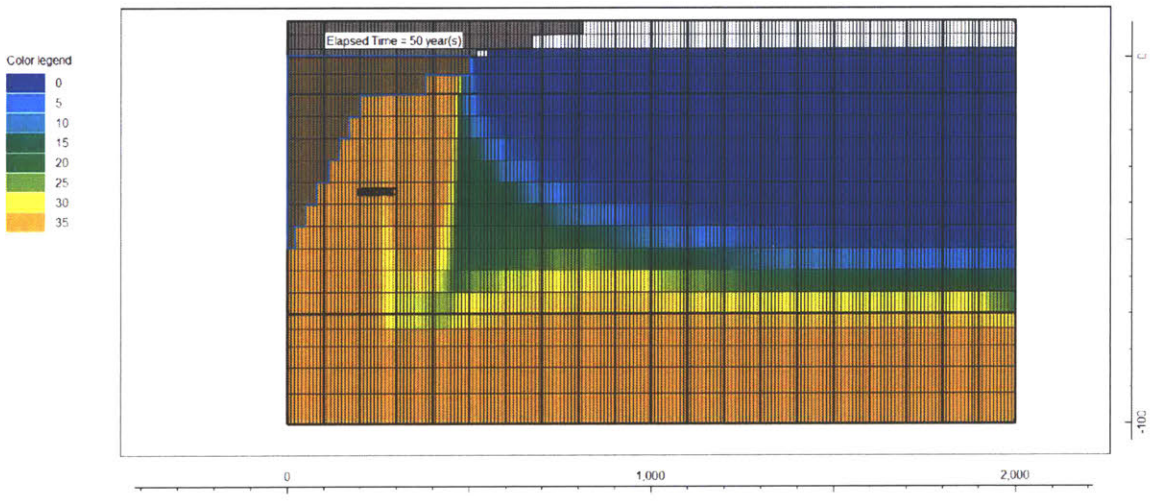

Figure 4-9: Salinity profile with the higher 5000 m^3/d extraction rate, year 50

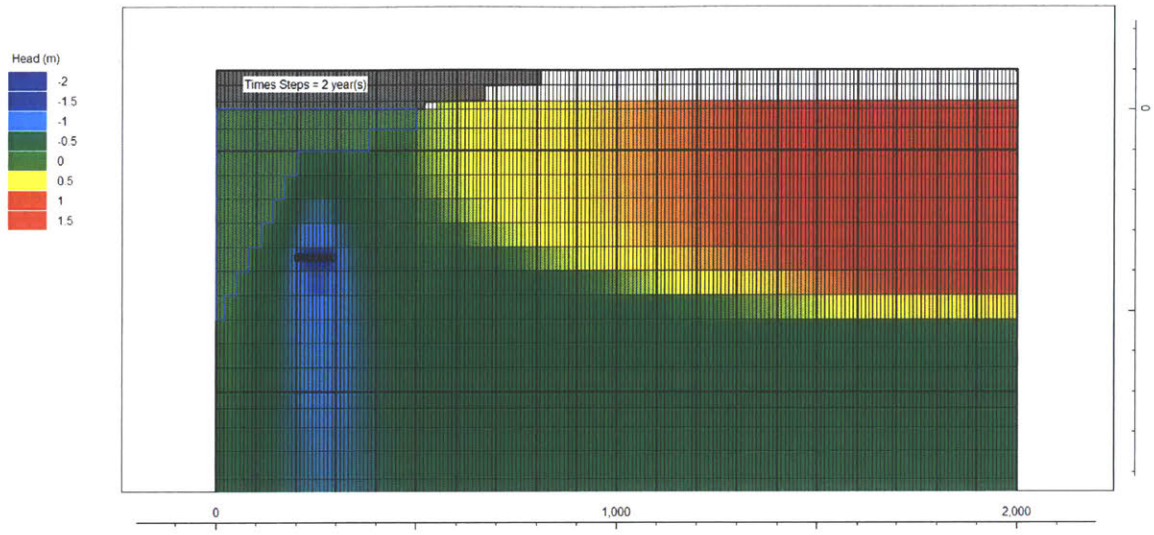

Figure 4-10: Head profile with the higher 5000 $^{m^3}/_{d}$ extraction rate, year 2

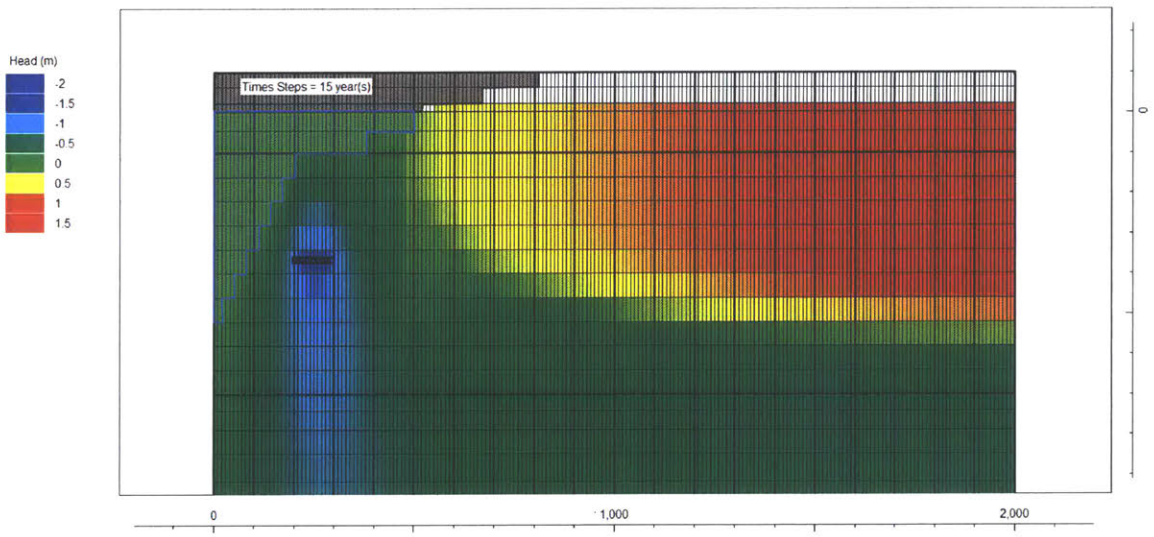

Figure 4-11: Head profile with the higher 5000 $^{m^3}/_{d}$ extraction rate, year 15

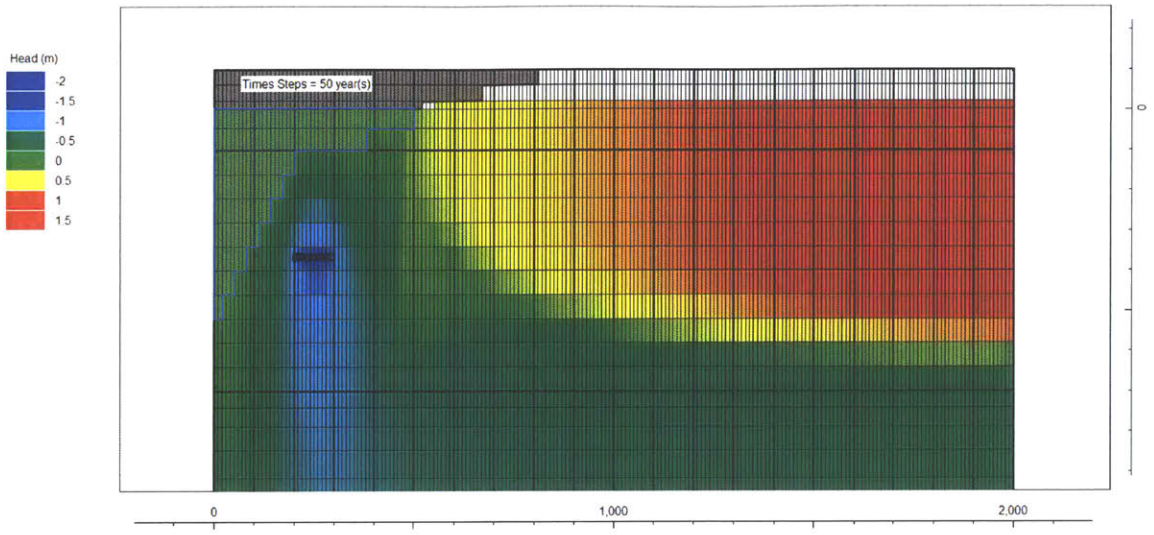

Figure 4-12: Head profile with the higher 5000 $^{m^3}/_{d}$ extraction rate, year 50

Chapter 5

Model results for brine injection

The MODFLOW well-package is used to model the injection pumps. 10 pumps were modeled across a 100m distance in the cross-shelf direction to simulate a single pump discharging to an injection well with 10 perforations. Using the initial condition of an existing freshwater lens, the model was ran for a total of 51 years, with one year of warm-up period with no injection, followed by 50 years of continuous brine injection. Different from extraction, the injected brine has twice the salinity of the feed water; as such, the injected brine was set to have a salinity of 70 PSU.

5.1 Injection rates and well locations

Extraction and Injection rates were determined based on two hypothetical desalination plants with freshwater production rates of 250 m^3/d and 2500 m^3/d. The production rate dictates the brine injection rate in relation to the production efficiency. In our case, the production rate has a 1:1 ratio to the injection rate of 250 m^3/d and 2500 m^3/d.

Although mass balance discrepencies increased when injection started due to sudden change in head gradients, it did not cause the simulation to terminate, implying that the convergence criteria were still met. This is an indicator that the problems cause in the extraction models may be related to the wetting option that determines whether cells switch between wet and dry. For the extraction model, a

significant number of cells turned dry; when the extraction wells are located further inland, which is also when the simulation experienced termination.

A total of 5 simulations were run for each injection rate at 5 locations across the cross-shelf direction between 250m inland from the coastline to 250m offshore, as shown below.

5.2 Brine, brackish, fresh water distribution

For the simulations with the low injection rate, the increased head due to injection is negligible such that the injected brine is transported by the ambient head, due to higher inland head, and dispersion. As seen in the profiles in figure 5-1 to 5-9, the freshwater lens was not disturbed during the entire duration of injection.

WIth the higher injection rate, the freshwater lens is pushed inland, but the freshwater lens is still largely intact, indicating the system can tolerate a higher injection rate. The results match closely with the intuition that, the further inland the wells are located, the more intrusion is caused. The results show that the brine does not demonstrate any significant sinking, implying that the flow of the brine is mostly governed by the increased head caused by the injection wells. Shown in Figures 5-1 to 5-9 are the salinity and head profiles for injection located about 50m inland from the coastline. Head profiles for the lower injection rate are excluded since the head changes are negligible. Results will be further discussed in Chapter 6.

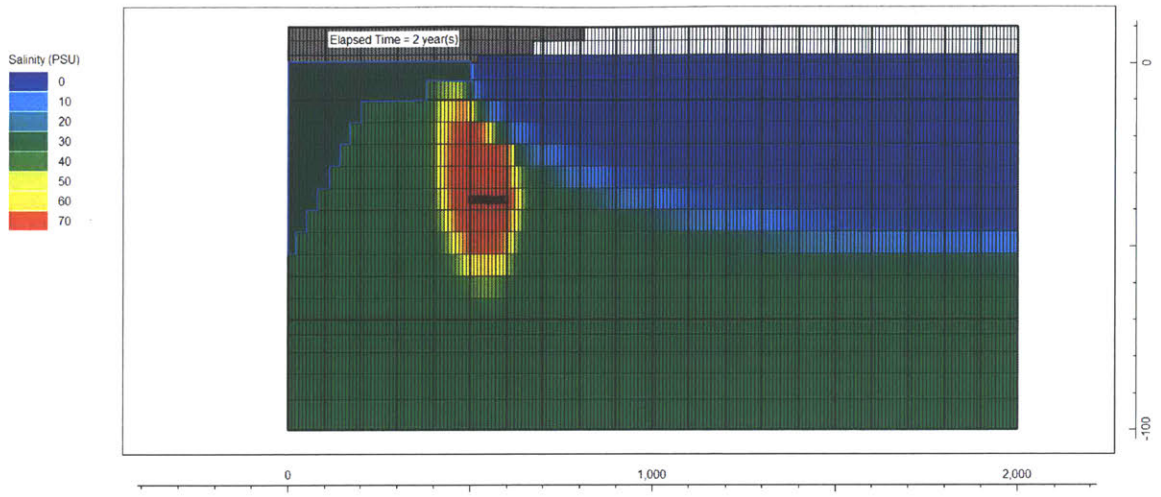

Figure 5-1: Salinity profile with the lower 250 m^3/d injection rate, year 2

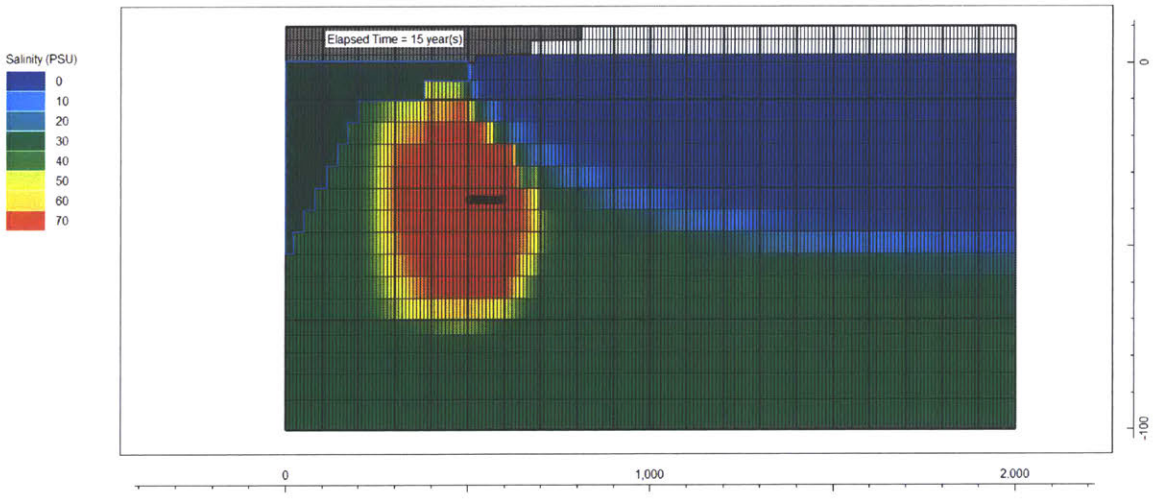

Figure 5-2: Salinity profile with the lower 250 m^3/d injection rate, year 15

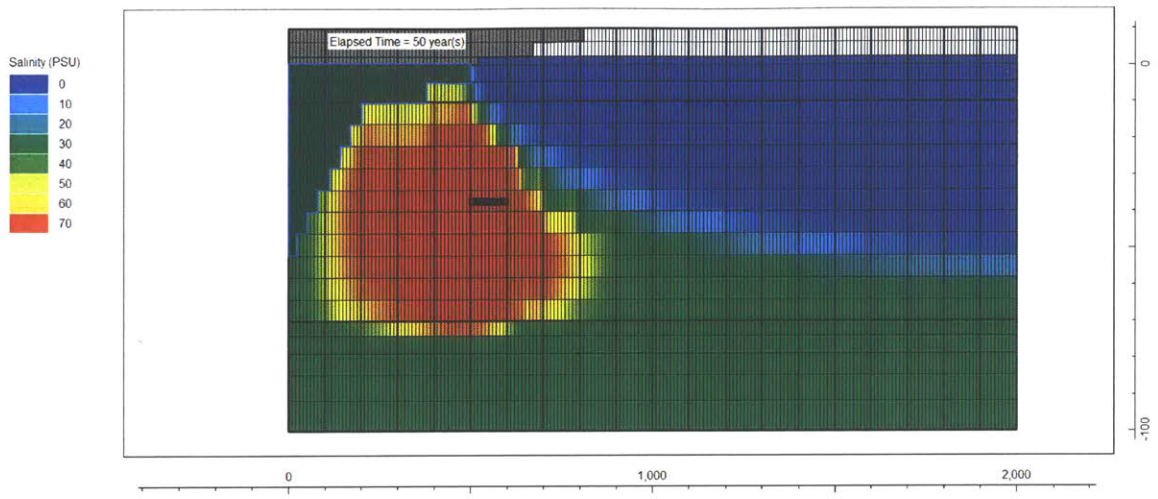

Figure 5-3: Salinity profile with the lower 250 $^{m^3}/_{d}$ injection rate, year 50

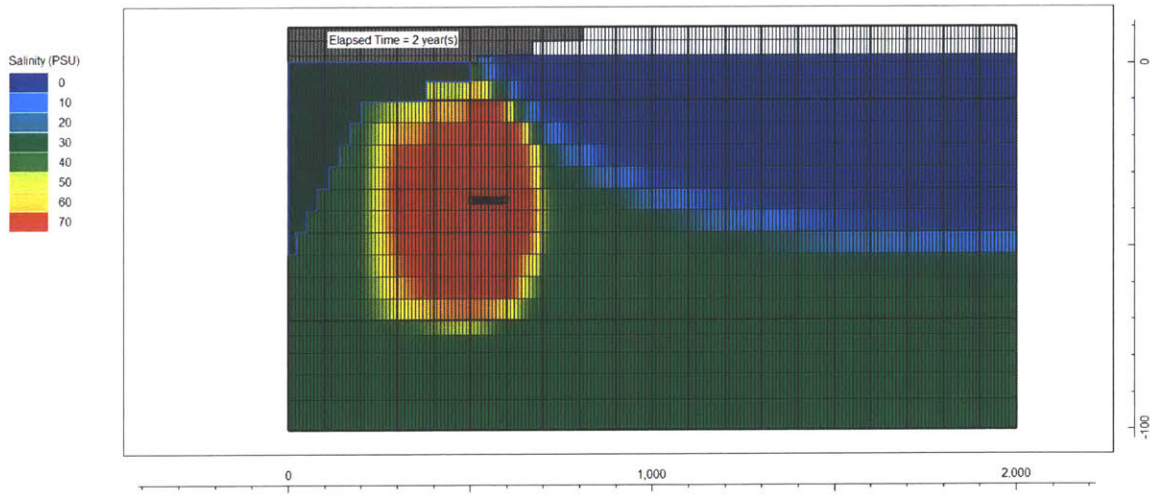

Figure 5-4: Salinity profile with the higher 2500 $^{m^3}/_{d}$ injection rate, year 2

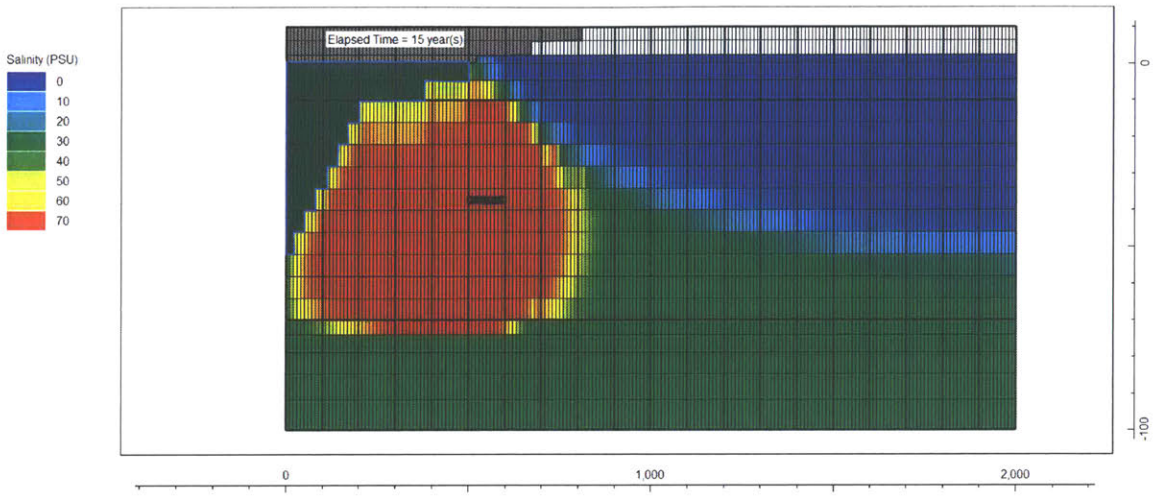

Figure 5-5: Salinity profile with the higher 2500 $^{m^3}/_{d}$ injection rate, year 15

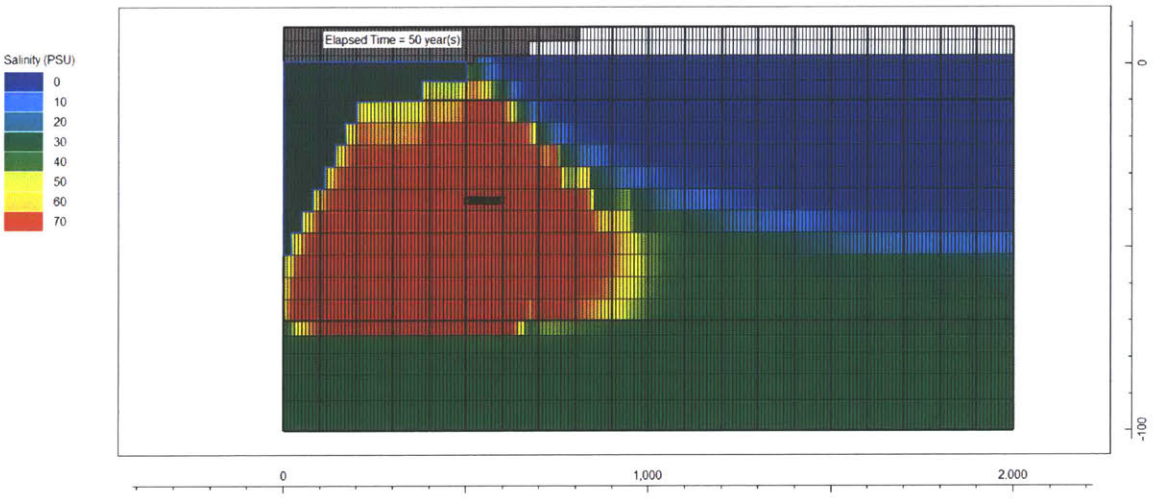

Figure 5-6: Salinity profile with the higher 2500 $^{m^3}/_{d}$ injection rate, year 50

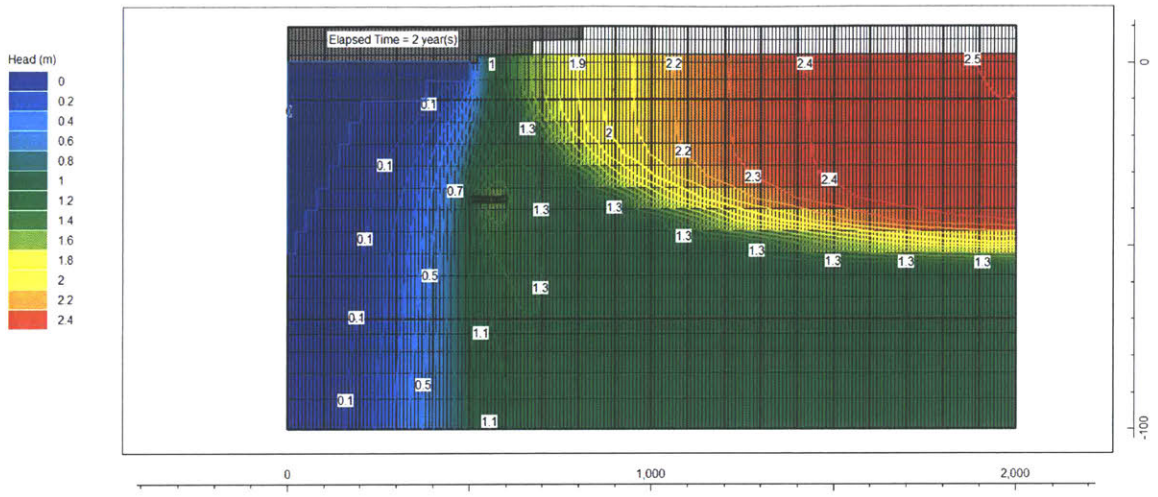

Figure 5-7: Head profile with the higher 2500 m^3/d injection rate, year 2

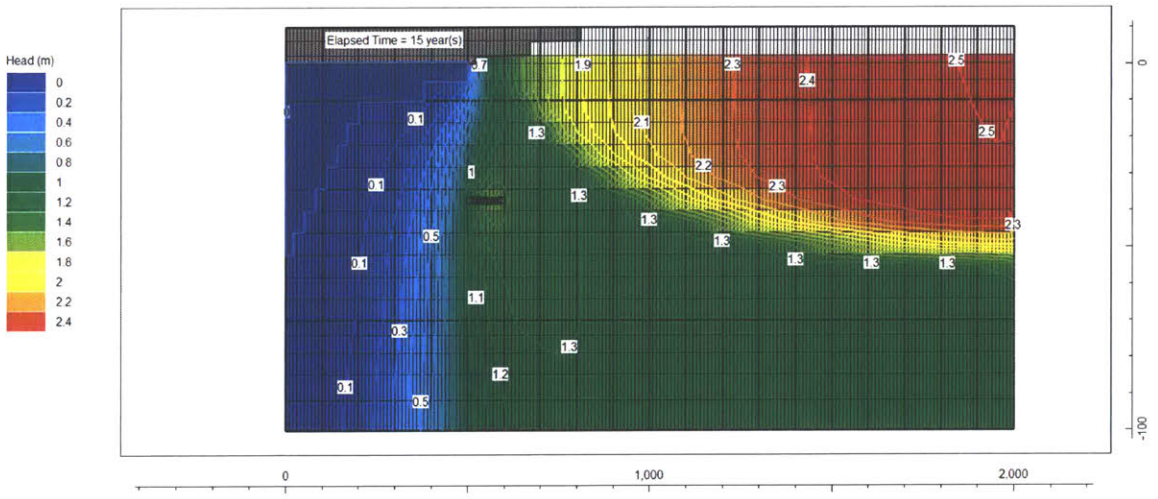

Figure 5-8: Head profile with the higher 2500 m^3/d injection rate, year 15

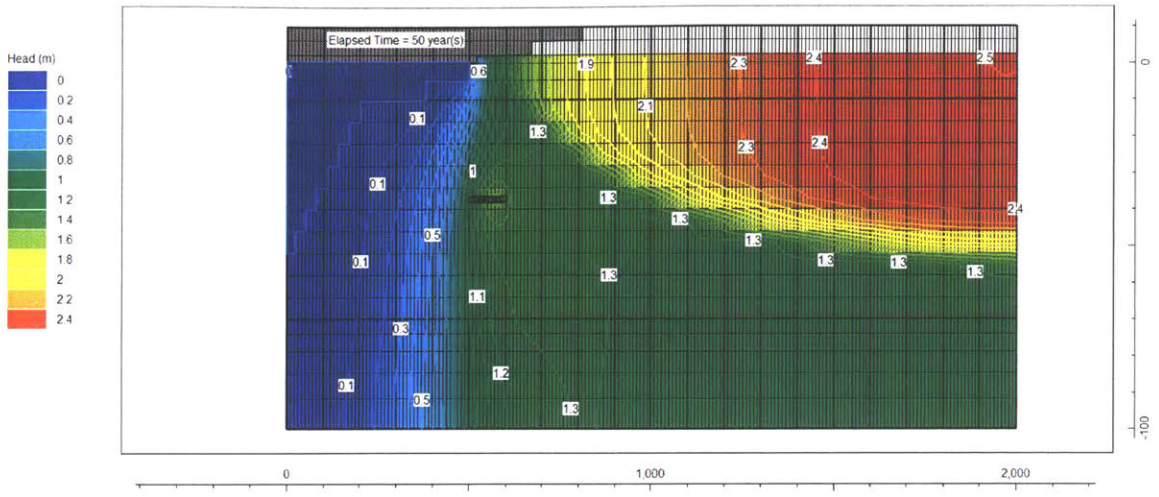

Figure 5-9: Head profile with the higher 2500 m^3/d injection rate, year 50

Chapter 6

Results and Discussion

6.1 Optimal locations for well systems

6.1.1 Extraction wells

Subsurface intakes generally require a higher construction and operation cost than conventional intakes. For a given set of hydrogeological conditions, a groundwater model can help determine an optimal location where the impact on existing freshwater storage can be minimized. At offshore extraction locations, the majority of the extracted water originates from the ocean, and the extracted freshwater flow should not be higher than the submarine discharged freshwater flow rate without extraction.

Figure 6-1 and 6-2 are two charts plotting the salinities of the extracted water for both low and high extraction rate for 10 extraction locations. A positive x distance denotes the inland distance from the coastline, whereas a negative x denotes the offshore distance from the coastline. For the low extraction rate, extraction has minimal impact to the freshwater lens starting at an offshore distance of 50m. When the extraction well is moved inland, seawater begins to intrude. Because the extraction rate is low, a steady-state brackish water salinity can be maintained, starting at the inland extraction location of 350m. The freshwater rate being extracted is equal to the recharge rate, and a same steady-state concentration

around 22 PSU is reached based on equation 3.5. For the higher extraction rate (Figure 6-2), the extraction rate exceeds the recharge rate, so for inland locations the salinities of the extracted water approaches 35 PSU.

For the theoretical system we modeled, the optimal extraction location is around 50 to 100m offshore. A more inland location will increase seawater intrusion.

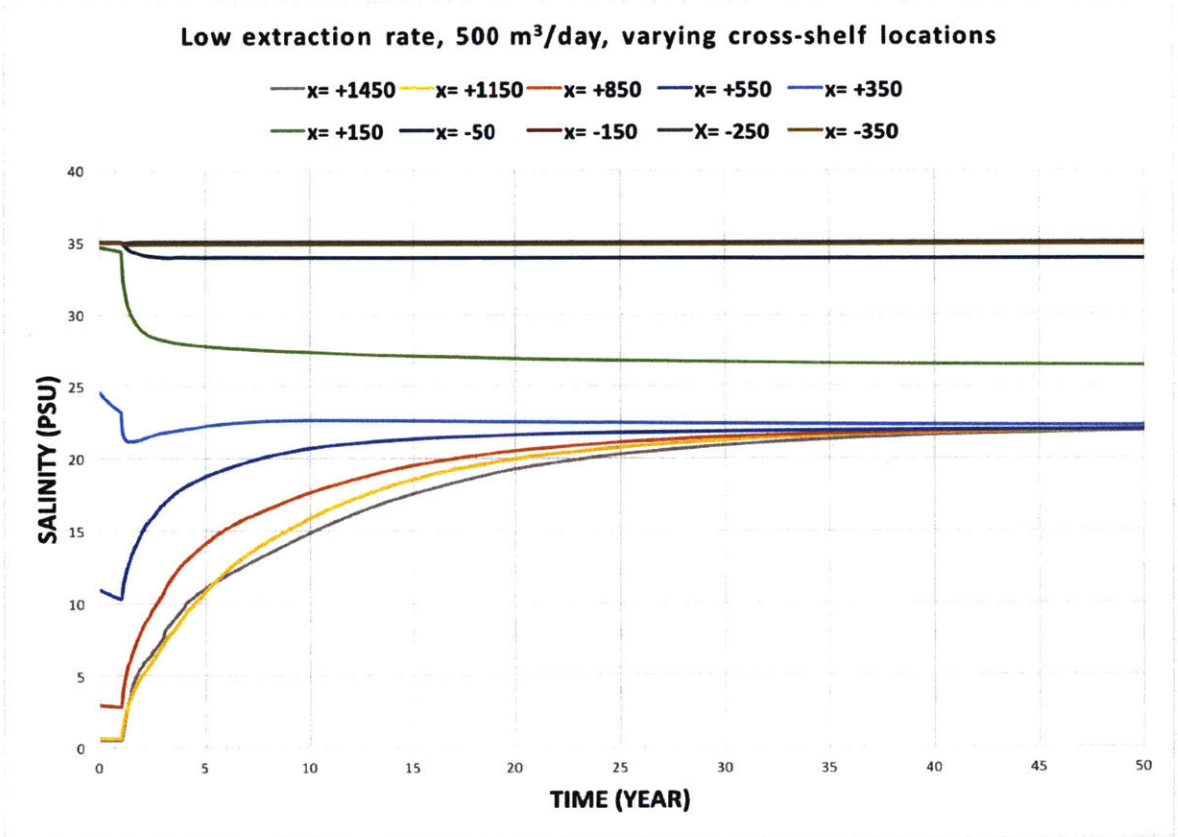

Figure 6-1: Salinity time-series low extraction rate, 500 $^{m^3}/_{d}$

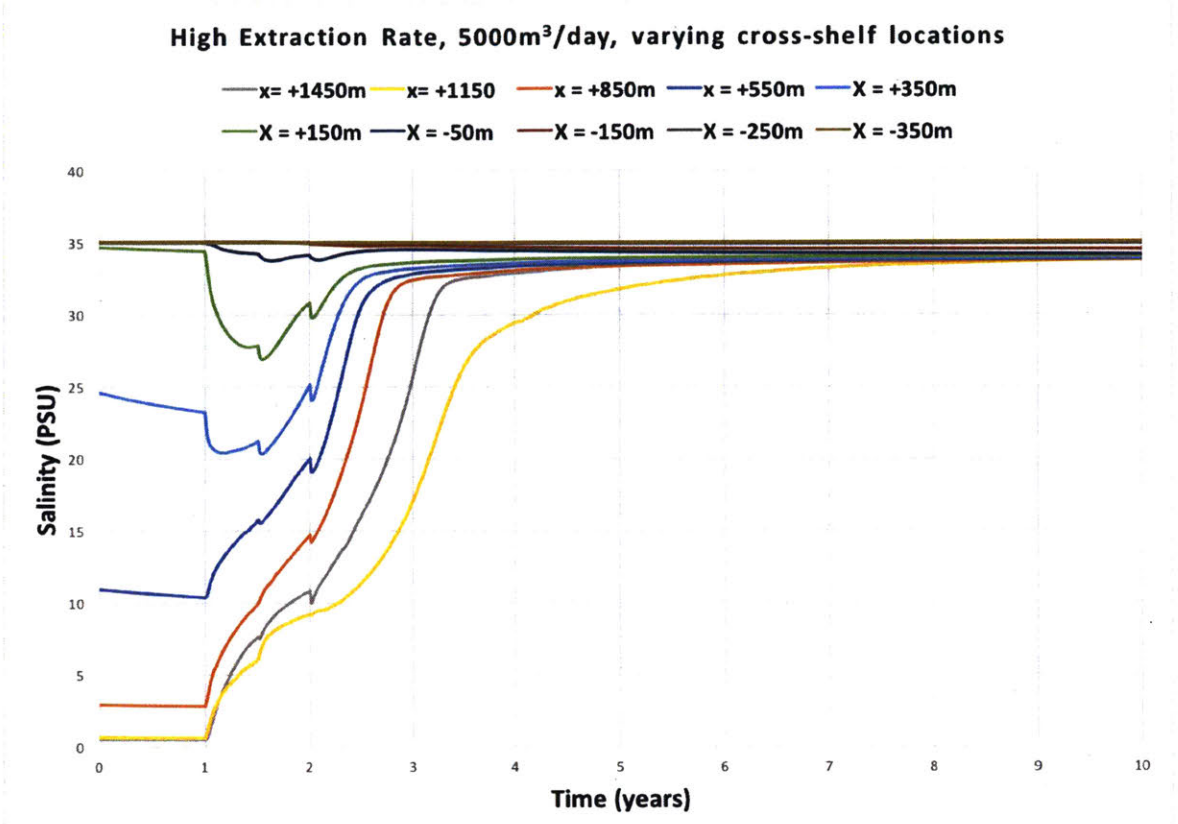

Figure 6-2: Salinity time-series high extraction rate, 5000 $^{m^3}/_{d}$

6.1.2 Injection wells

Comparing to extraction, injection has less impact on the interaction of desalination plant with freshwater. Results show that even with the higher injection rate of 2500 $^{m^3}/_{d}$, the freshwater lens is still largely intact. However, this may be a result of the modeled ocean boundary having a high conductance, meaning that the sediment layer on the seafloor does not restrict the exchange of seawater and brine at the sea floor. For a desalination plant with subsurface extraction wells, some studies have shown that the extraction head may lead to the accumulation of natural organic matter on the sea floor[13]. Over time, the decomposed organic matter in the sediment can lower the conductance of the ocean boundary, thus reducing the dilution of seawater and brine, and causing the injected brine to push further inland.

6.2 Test models comparison

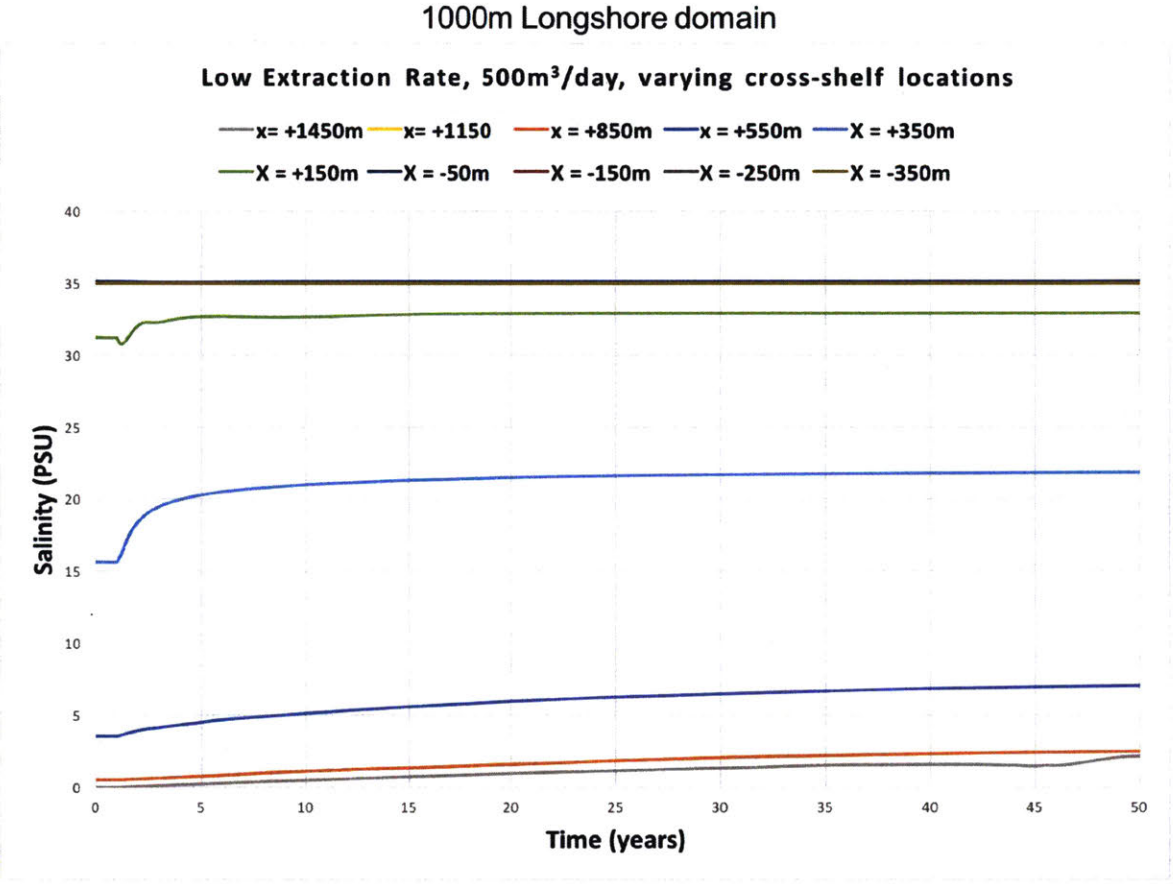

Figure 6-3: 2D model, salinity time-series low extraction rate, 500 $^{m^3}/_{d}$, 1000m uniform longshore

Figure 6-3 shows the time-varying salinities for the first test model with a uniform 1000m longshore domain. Compared with the base models, this test model is also two dimensional but has less extraction than inflow. Results show that the extraction well located at 350m inland experienced the greatest salinity change during the 50 years of extraction. This particular well is located in the middle of the brackish water zone, and the slightest head gradient will cause the brackish water to shift. The salinity of the extracted water in other wells has much smaller changes, which is a good indicator that the extraction activity has negligible effect on the freshwater storage. The results also agree with the fact that the, because recharge rate ($0.47^{m}/_{yr} \times 1500000m^2 \div 365^{d}/_{yr} \approx 2000^{m^3}/_{d}$) is much larger than the extraction rate (500 $^{m^3}/_{d}$),

there is adequate supply of freshwater without depleting the freshwater storage.

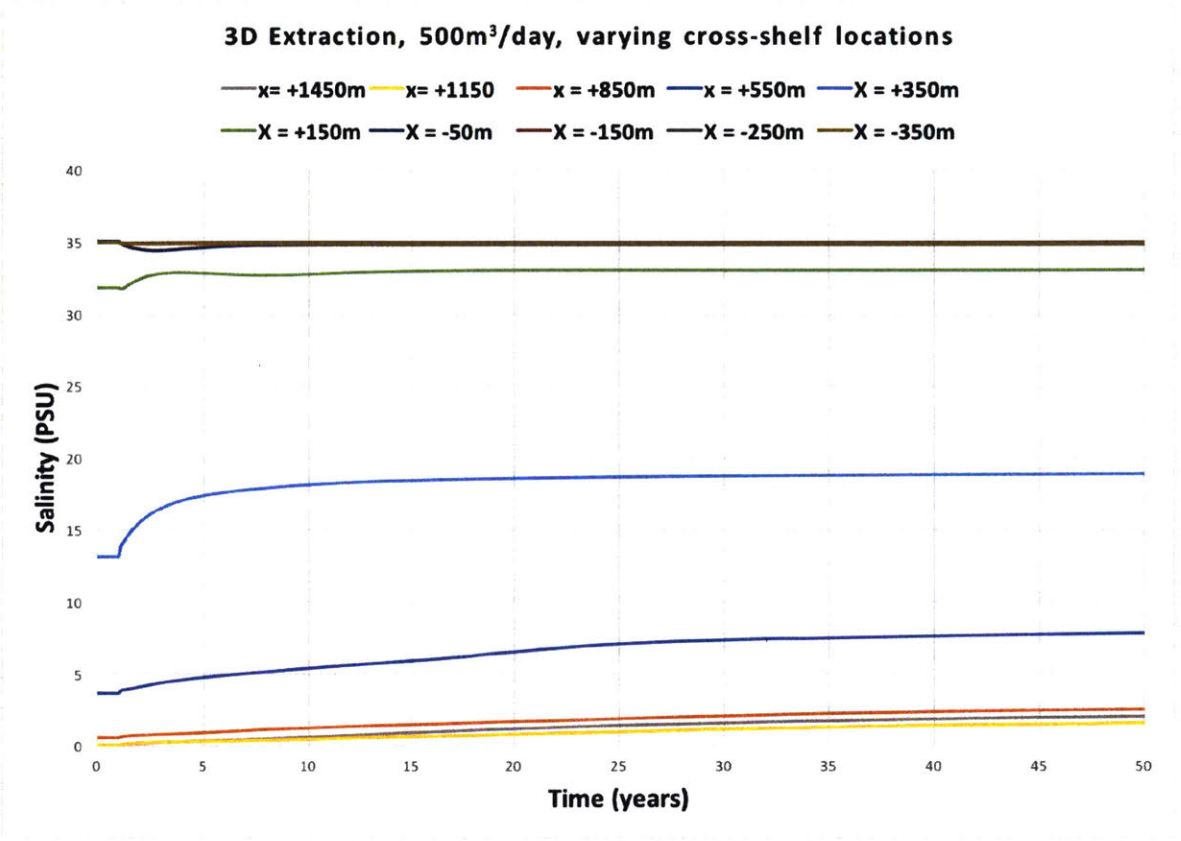

Figure 6-4: 3D model, salinity time-series local extraction rate, 500 $^{m^3}/_{d}$

Figure 6-4 shows the results for the 3D test model. For this test model, we expected seawater intrusion to be more prominent when compared to the first test model, but not as severe when compared to the base models with the same extraction rate. The centrally located extracted well is located at mid-width in the longshore direction, over a distance of 10m (one-tenth of the longshore domain, see Figure 3-7). The 3D model demonstrates that the extraction induces stronger head gradients locally around the well in the beginning of extraction, but very quickly transitions into a 2D simulation as the drawdown from extraction reaches the longshore boundaries; hence the time-varying salinities largely resemble the trend shown in Figure 6-3. This is because both test models have the same recharge-extraction ratio of: $Q_{recharge}/Q_{extraction} \approx 4$.

6.3 Future Projects

The model parameters are idealized with reference to real-word scenarios. It would be helpful to validate the model at desalination plant locations with known hydrogeological conditions, and also determine whether it is necessary to model the aquifer in 3D.

The same model can also be tested using other groundwater modeling codes to compare discrepencies of modeling performance. SUTRA requires a longer model setup time but is capable of checking energy balances. Professor Charles Harvey at the Parsons Laboratory is particularly interested in this topic as he realizes that, at times, energy may not be conserved even when mass balance is conserved in groundwater models.

The seawater pocket as seen in the extraction model may be a result of modeling errors. A better understanding of the mixing processes can help to determine whether the results we see are physcial possible.

Appendix A

SEAWAT VDF codes

-1	1	-1	1	MT3DRHOFLG	MFNADVFD	NSWTCPL	IWTABLE
1000.0000		1025.0000		DENSEMIN		DENSEMAX	
0.000				DNSCRIT			
1000.0000	0.00446	0.000		DENSEREF	DRHODPRHD	PRHDREF	
1				NSRHOEOS			
1	0.7143	0		MTRHOSPEC(1)	DRHODC(1)	CRHOREF(1)	
1.0000e-02				FIRSTDT			

An excerpt from [12] below explains the above parameters for the SEAWAT VDF Input File.

MT3DRHOFLG - is the MT3DMS species number that will be used in the equation of state to compute fluid density. This input variable was formerly referred to as MTDNCONC (Langevin and others, 2003). If MT3DRHOFLG = 0, fluid density is specified using items 6 and 7, and flow will be uncoupled with transport if the IMT Process is active. If MT3DRHOFLG > 0, fluid density is calculated using the MT3DMS species number that corresponds with MT3DRHOFLG. A value for MT3DRHOFLG greater than zero indicates that flow will be coupled with transport. If MT3DRHOFLG = -1, fluid density is calculated using one or more MT3DMS species. Items 4a, 4b, and 4c will be read instead of item 4. The dependence of fluid density on pressure head can only be activated when MT3DRHOFLG = -1. A value for MT3DRHOFLG of -1 indicates that flow will be coupled with transport.

MFNADVFD - is a flag that determines the method for calculating the internodal density values used to conserve fluid mass. If MFNADVFD = 2, internodal conductance values used to conserve fluid mass are calculated using a central-in-space algorithm. If MFNADVFD $\neq$ 2, internodal conductance values used to conserve fluid mass are calculated using an upstream-weighted algorithm.

NSWTCPL - is a flag used to determine the flow and transport coupling procedure. If NSWTCPL = 0 or 1, flow and transport will be explicitly coupled using a one-timestep lag. The explicit coupling option is normally much faster than the iterative option and is recommended for most applications. If NSWTCPL > 1, NSWTCPL is the maximum number of non-linear coupling iterations for the flow and transport solutions. SEAWAT-2000 will stop execution after NSWTCPL iterations if convergence between flow and transport has not occurred. If NSWTCPL = -1, the flow solution will be recalculated only for: The first transport step of the simulation, or The last transport step of the MODFLOW timestep, or The maximum density change at a cell is greater than DNSCRIT.

IWTABLE - is a flag used to activate the variable-density water-table corrections (Guo and Langevin, 2002, eq. 82). If IWTABLE = 0, the water-table correction will not be applied. If IWTABLE > 0, the water-table correction will be applied.

DENSEMIN - is the minimum fluid density. If the resulting density value calculated with the equation of state is less than DENSEMIN, the density value is set to DENSEMIN. Input Instructions and Evaluation of Temperature Output 17 18 SEAWAT Version 4: A Computer Program for Simulation of Multi-Species Solute and Heat Transport If DENSEMIN = 0, the computed fluid density is not limited by DENSEMIN (this is the option to use for most

simulations). If DENSEMIN > 0, a computed fluid density less than DENSEMIN is automatically reset to DENSEMIN.

DENSEMAX - is the maximum fluid density. If the resulting density value calculated with the equation of state is greater than DENSEMAX, the density value is set to DENSEMAX. If DENSEMAX = 0, the computed fluid density is not limited by DENSEMAX (this is the option to use for most simulations). If DENSEMAX > 0, a computed fluid density larger than DENSEMAX is automatically reset to DENSEMAX.

DNSCRIT - is a user-specified density value. If NSWTCPL is greater than 1, DNSCRIT is the convergence crite- rion, in units of fluid density, for convergence between flow and transport. If the maximum fluid density difference between two consecutive implicit coupling iterations is not less than DNSCRIT, the program will continue to iterate on the flow and transport equations, or will terminate if NSWTCPL is reached. If NSWTCPL is -1, DNSCRIT is the maximum density threshold, in units of fluid density. If the fluid density change (between the present transport timestep and the last flow solution) at one or more cells is greater than DNSCRIT, then SEAWAT_V4 will update the flow field (by solving the flow equation with the updated density field).

DENSEREF - is the fluid density at the reference concentration, temperature, and pressure. For most simulations, DENSEREF is specified as the density of freshwater at 25 C and at a reference pressure of zero.

DRHODPRHD - is the slope of the linear equation of state that relates fluid density to the height of the pressure head (in terms of the reference density). Note that DRHODPRHD can be calculated from the volumetric expan- sion coefficient for pressure using equation 15. If the simulation is formulated in terms of kilograms and meters, DRHODPRHD has an approximate value of 4.46 x 10-3 kg/m4. A value of zero, which is typically used for most problems, inactivates the dependence of fluid density on pressure.

PRHDREF - is the reference pressure head. This value should normally be set to zero.

NSRHOEOS - is the number of MT3DMS species to be used in the equation of state for fluid density. This value is read only if MT3DRHOFLG = -1.

MTRHOSPEC - is the MT3DMS species number corresponding to the adjacent DRHODC and

CRHOREF.

DRHODC - formerly referred to as DENSESLP (Langevin and others, 2003), is the slope of the linear equation of state that relates fluid density to solute concentration. In SEAWAT_V4, separate values for DRHODC can be entered for as many MT3DMS species as desired. If DRHODC is not specified for a species, then that species does not affect fluid density. Any measurement unit can be used for solute concentration, provided DENSEREF and DRHODC are set properly. DRHODC can be approximated by the user by dividing the density difference over the range of end- member fluids by the difference in concentration between the end-member fluids.

CRHOREF - is the reference concentration (C0) for species, MTRHOSPEC. For most simulations, CRHOREF should be specified as zero. If MT3DRHOFLG $>$ 0, CRHOREF is assumed to equal zero (as was done in previous versions of SEAWAT).

FIRSTDT - is the length of the first transport timestep used to start the simulation if both of the following two condi- tions are met: 1. The IMT Process is active, and 2. Transport timesteps are calculated as a function of the user-specified Courant number (the MT3DMS input variable, PERCEL, is greater than zero).

Appendix B

SEAWAT Model Structure Flowchart

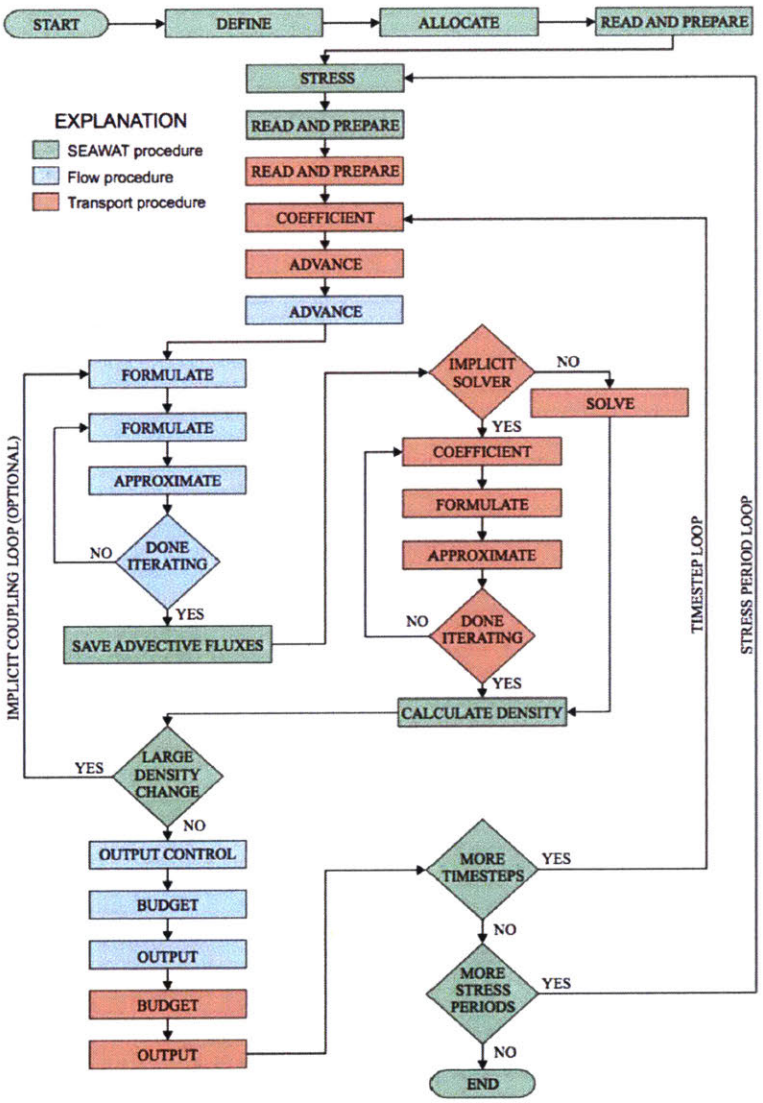

Figure B-1: Illustration of the Ghyben-Herzberg relation in a coastal aquifer[9]

Bibliography

[1] Samir Al-Mashharawi, Abdullah H.a. Dehwah, Khaled Bin Bandar, and Thomas M. Missimer. Feasibility of using a subsurface intake for SWRO facility, south of Jeddah, Saudi Arabia. *Desalin. Water Treat.*, (November 2014):1–11, 2014.

[2] Gary Amy, Noreddine Ghaffour, Zhenyu Li, Lijo Francis, Rodrigo Valladares Linares, Thomas Missimer, and Sabine Lattemann. Membrane-based seawater desalination: Present and future prospects. *Desalination*, 401:16–21, 2017.

[3] Phatcharasak Arlai and Manfred Koch. The Importance of Density Dependent Flow and Solute Transport Modeling to simulate Seawater Intrusion into a Coastal ... (August):3–5, 2015.

[4] Paul M Barlow. Ground Water in Freshwater-Saltwater Environments of the Atlantic Coast. *U S Geol. Surv. - Circ. 1262*, Circular 1:121, 2003.

[5] PAUL M. BARLOW and EMILY C. WILD. Bibliography on the Occurrence and Intrusion of Saltwater in Aquifers along the Atlantic Coast of the United States Intrusion of Saltwater in Aquifers along the Atlantic Coast of the United States. Technical report.

[6] Heather Cooley, Newsha Ajami, and Matthew Heberger. KEY ISSUES IN SEAWATER DESALINATION IN CALIFORNIA: Marine Impacts. page 32, 2013.

[7] Abdullah H A Dehwah and Thomas M. Missimer. Subsurface intake systems: Green choice for improving feed water quality at SWRO desalination plants, Jeddah, Saudi Arabia. *Water Res.*, 88:216–224, 2016.

[8] DHI-WASY. FEFLOW 7.0 Use Guide. page 124, 2015.

[9] Weixing Guo and Christian D. Langevin. *User's Guide to SEAWAT: A computer program for simulation of three-dimensional variable-density ground-water flow.* Number Book 6. 2002.

[10] P Kumar C and Surjeet Singh. Concepts and Modeling of Groundwater System. *Int. J. Innov. Sci. Eng. Technol.*, 2(2):262–271, 2015.

[11] Christian D. Langevin. Simulation of Ground-Water Discharge to Biscayne Bay, Southeastern Florida. *United States Geol. Surv.*, pages 1–127, 2001.

[12] Christian D. Langevin, Daniel T. Thorne Jr., Alyssa M. Dausman, Michael C. Sukop, and Weixing Guo. SEAWAT Version 4: A Computer Program for Simulation of Multi-Species Solute and Heat Transport. *U.S. Geol. Surv. Tech. Methods B. 6*, page 39, 2007.

[13] Erin D. Mackey, Nicki Pozos, Wendie James, Tom Seacord, Henry Hunt, and David L. Mayer. *Assessing Seawater Intake Systems for Desalination Plants.* 2011.

[14] Robert G. Maliva, Thomas M. Missimer, and Russell Fontaine. Injection Well Options for Sustainable Disposal of Desalination Concentrate. *IDA J. Desalin. Water Reuse*, 3(3):17–23, 2011.

[15] M L Merritt. Simulation of the water-table altitude in the Biscayne aquifer, southern Dade County, Florida, water years 1945-89. *US Geol. Surv. Water Supply Pap.*, 2458:1–148, 1996.

[16] Thomas M. Missimer, Noreddine Ghaffour, Abdullah H A Dehwah, Rinaldi Rachman, Robert G. Maliva, and Gary Amy. Subsurface intakes for seawater reverse osmosis facilities: Capacity limitation, water quality improvement, and economics. *Desalination*, 322:37–51, 2013.

[17] Ann E Mulligan, Christian Langevin, and Vincent E A Post. Tidal Boundary Conditions in SEAWAT. *Ground Water*, 49(6):866–879, 2011.

[18] For Immediate Release and State Water Board. Y our W ater B irth. pages 8630–8630, 2015.

[19] Saif Uddin. Environmental Impacts of Desalination Activities in the Arabian Gulf. *Int. J. Environ. Sci. Dev.*, 5(2), 2014.

[20] Đą.I. Voss and A.M. Provost. SUTRA: a model for saturated-unsaturated, variable-density ground-water flow with solute or energy transport. *Water-Resources Investig. Rep. 02-4231*, 2010:300 p, 2010.

[21] WateReuse Association. Desalination Plant Intakes Impingement and Entrainment Impacts and Solutions. (June), 2011.